# Investigation of the role of the AP2/ERF transcription factor ERN1 in the root nodule symbiosis signaling network of *Lotus japonicus*

(根粒共生の情報伝達ネットワークにおける

ミヤコグサ AP2/ERF 転写因子 ERN1 の役割)

**Liu, Meng**

**Department of Basic Biology, School of Life Science**

**SOKENDAI (The Graduate University for Advanced Studies)**

**Submission date: 01 OCT 2019**

**Declaration: This dissertation is submitted for the degree of Doctor of Philosophy**

# DEDICATION

To the memory of my grandmother, for her unconditional love.

# ACKNOWLEDGEMENT

# TABLE OF CONTENTS

# ABBREVIATIONS

| | |
|---|---|
| 6-BA | 6-benzylaminopurine |
| CCaMK | Calcium and Calmodulin-Dependent Protein Kinase |
| CLE-RS | CLE Root Signal |
| DEGs | Differentially expressed genes |
| DMI | Doesn't Make Infections |
| dpi | days post infection |
| Epr3 | Exopolysaccharide Receptor 3 |
| ERN1 | ERF REQUIRED FOR NODULATION 1 |
| EXPB2 | β-Expansin gene 2 |
| FC | Fold change |
| FDR | False discovery rate |
| FH8 | Formin homolog 8 |
| HMGR1 | 3-Hydroxy-3-Methylglutaryl CoA Reductase 1 |
| IPD3 | INTERACTING PROTEIN OF DMI3 |
| IT | Infection thread |
| *L. japonicus* | *Lotus japonicus* |
| MC | Micro-colony |
| *M. loti* | *Mesorhizobium loti* |
| *M. truncatula* | *Medicago truncatula* |
| MVA | Mevalonate |
| NFR | Nod factor receptor |

| | |
|---|---|
| NF-YA1 | Nuclear Factor-YA1 |
| NIN | NODULE INCEPTION |
| Nod factor | Nodulation factor |
| NPL | NODULATION PECTATE LYASE |
| NSP1 | NODULATION SIGNALING PATHWAY 1 |
| PCA | Principal component analysis |
| qRT-PCR | Quantitative real-time PCR |
| RopGEF3 | Rho GTPase guanine nucleotide exchange factor 3 |
| SCARN | SCAR-Nodulation |
| SYMRK | Symbiosis Receptor-like Kinase |
| WT | Wild type |

# 1. GENERAL INTRODUCTION

Nitrogen is critical for plant growth, as it is a basic component of amino acids, nucleic acids, and other biomolecules. However, the availability of nitrogen in soil is limited. Plants have developed strategies to overcome this nutritional deficiency, such as modification of the root architecture and recycling of nitrogen from senescent organs. An additional strategy is root nodule symbiosis, which utilizes bacterial enzyme nitrogenase to catalyze the conversion of atmospheric $N_2$ to $NH_3$, a usable form of nitrogen for plants. Two main root nodule symbiosis systems are known between plants and nitrogen-fixing soil bacteria; a variety of woody dicotyledonous plants (termed actinorhizal plants) interact with *Frankia*, and legumes in the *Fabaceae* family (as well as the non-legume *Parasponia*) are associated with rhizobia (Beauchemin et al. 2015; Svistoonoff et al. 2015). In both systems, symbiotic bacteria induce the formation of a unique organ, termed a root nodule. The microsymbionts are accommodated in nodule cells and fix nitrogen, while their carbon source is supplied by the host plant (Pawlowski and Demchenko 2012). Root nodule symbiosis confers plants with a considerable growth advantage in nitrogen-limited conditions and is agriculturally valuable.

The legume-rhizobium symbiosis is better understood because of its valuable contribution to agriculture and advantages for laboratory applications. In this system, the formation of a root nodule involves two synchronized processes: 1) rhizobial infection through the root epidermis into the cortex (Figure 1a−d) and 2) nodule primordium formation initiated by several cortical cells re-entering the cell cycle underneath the infection foci (Figure 1c−e). Two types of nodules are formed in legume roots, namely indeterminate and determinate nodules (Hirsch 1992). Indeterminate nodules contain a meristem at the nodule apex that continuously produces new cells for apical growth. In

determinate nodules, the meristem is only transiently present. *Medicago truncatula* and *Lotus japonicus* are two model legumes representing plants that form indeterminate and determinate root nodules, respectively.

The following two sections introduce the process of rhizobial invasion of the host and the signaling pathways regulating the host response.

## 1.1 Rhizobia invade the host legume and induce root nodule formation

Rhizobia gain entry into the host root using two major strategies: entry through cracks in the root epidermis where lateral roots emerge and intracellular invasion through root hairs. Many legumes, such as the model species *L. japonicus* and *M. truncatula*, have adopted the intracellular approach (Guinel and Geil 2002). For intracellular invasion, rhizobial infection is initiated through the molecular dialog between the two partners; the rhizobia sense certain flavonoids released from leguminous roots and produce lipo-chitooligosaccharide nodulation signaling molecules (Nod factors; Figure 1a). The variation in chemical structure of Nod factors is critical to determine the compatibility between rhizobia and host legumes. Host recognition of Nod factors triggers root hair deformation, which is an early, essential step for establishment of this symbiotic relationship, and is followed by the invasion of bacteria into the inner tissues of the host root (reviewed by Oldroyd 2013).

When compatible rhizobia attach to the surface of host root hair, the Nod factors produced by rhizobia induce swelling of the root hair tip, re-initiation of apical growth, resulting in formation of a "shepherd's crook" structure (Figure 1a, b). Rhizobia entrapped in the crook of the root hair multiply and form micro-colonies (MCs). Rhizobia then penetrate the root hair via infection threads (ITs; Figure 1c), the tubular invaginations of the host cell wall and plasma membrane (Ardourel et al. 1994). Infection threads filled with growing, dividing rhizobia elongate toward the base of the root hair (Figure 1c).

2

Concomitant with progression of infection in the epidermis, root cortical cells re-enter the cell cycle, giving rise to the nodule primordium (Figure 1c, d; van Spronsen et al. 2001). After infection threads exit from the epidermal cell, bacteria enter the space between the epidermal and cortical cell layers. Invagination−similar to the process in root hairs−starts in the cortical cell layer. Infection threads grow toward the dividing cortical cells and ramify (Figure 1d). Rhizobia are then released from the infection threads into nodule cells. Rhizobia are enclosed in a peribacteroid membrane derived from the host plasma membrane (Figure 1e, f). Finally, the rhizobia differentiate into bacteroids and acquire the ability for nitrogen fixation (Gage 2004; Kouchi et al. 2010). Therefore, the initiation and development of infection threads from root hairs to the cortex are critical for a successful and efficient infection.

## 1.2 Nod factor signaling pathway leads to gene reprograming in the nucleus

The symbiotic responses in root hairs are regulated by signal transduction. An overview of components in the root nodule symbiosis pathway is presented in Figure 2 (Oldroyd 2013; Downie 2014). The Nod factors produced by rhizobia are perceived by Nod factor receptors (NFR) on the cell membrane (Figure 2a). A suite of Lysin motif (LysM) receptor-like kinases have been identified in *L. japonicus* and *M. truncatula* as Nod factor receptors, including LjNFR1/ MtLYK3, LjNFR5/ MtNFP, and LjNFRe (Amor et al. 2003; Limpens et al. 2003; Madsen et al. 2003; Radutoiu et al. 2003; reviewed by Kelly et al. 2017; Murakami et al. 2018). Biochemical assays have shown that LjNFR1, LjNFR5, and LjNFRe bind Nod factors with high affinity (Broghammer et al. 2012; Murakami et al. 2018). Mutations of LjNFR1/ MtLYK3 and LjNFR5/ MtNFP block symbiotic responses to infection, including root hair deformation and expression of early nodulation genes. LjNFR1 and LjNFRe can form heterodimers with LjNFR5 and phosphorylate the LjNFR5 cytoplasmic domain

(Madsen et al. 2011; Murakami et al. 2018). Rho of Plants (ROP) GTPase 6 in *L. japonicus* interacts with LjNFR5 and is suggested to be involved in the regulation of root hair deformation (Ke et al. 2012). LjNFR5 also associates with a Leucine-rich repeat (LRR) receptor kinase Symbiosis Receptor-like Kinase (LjSYMRK). *symrk* mutants respond to rhizobial infection and display root hair swelling and branching but do not form infection threads (Endre et al. 2002; Stracke et al. 2002). LjSYMRK is suggested to be a critical link that connects Nod factor perception with early gene responses. In *M. truncatula*, Doesn't Make Infections 2 (DMI2), the ortholog of LjSYMRK, interacts with 3-Hydroxy-3-Methylglutaryl CoA Reductase 1 (HMGR1), a key enzyme regulating mevalonate (MVA) production. MVA can elicit expression of an early nodulation gene (nodulin; *MtENOD11*) and $Ca^{2+}$ spiking similar to that observed when Nod factors are applied in *M. truncatula* root hairs. A role for MVA in transmitting the nodulation signal from the plasma membrane to the nucleus has been suggested (Venkateshwaran et al. 2015). Nod factor receptors and their associating proteins constitute a platform for mediating Nod factor recognition, phosphorylation cascades at the plasma membrane, and subsequent signal transmission (Yoshida and Parniske, 2005; reviewed by Oldroyd and Downie, 2008).

Nod factor signaling activates expression of the LysM receptor *Exopolysaccharide receptor 3* (*LjEpr3*). LjEpr3 distinguishes compatible exopolysaccharides (EPS) produced by rhizobia. Similar to Nod factors, EPS also show strain-specific characteristics. LjEpr3 directly binds to EPS and regulates rhizobial passage through the host epidermal cell layer. Perception of the Nod factor and EPS constitute a two-step recognition mechanism to manage rhizobial infection. Nod factor signaling leads to rhizobial colonization of the curled root hair and infection thread initiation. LjEpr3 promotes persistence of rhizobial infection. Infection by rhizobia with incompatible EPS is blocked in short infection threads (Kawaharada et al. 2015).

Nod factor signaling triggers $Ca^{2+}$ oscillations in the nucleus via an undetermined secondary signal and nuclear membrane proteins, including several ion channels and nucleoporins (Figure 2b; Ehrhardt et al. 1996; Miwa et al. 2006). The $Ca^{2+}$ spiking is decoded by a calcium and calmodulin-dependent protein kinase (LjCCaMK; Figure 2c)/ DOESN'T MAKE INFECTIONS3 (MtDMI3) (Lévy et al. 2004; Tirichine et al. 2006). LjCCaMK plays a central role in signal transduction. The $Ca^{2+}$ ions bind to EF-hand motifs that are present in the regulatory region of LjCCaMK and induce its autophosphorylation, which subsequently enable calmodulin binding and substrate phosphorylation (Shimoda et al. 2012; Singh and Parniske 2012). *ljccamk* mutants exhibit root hair swelling and branching in response to Nod factor treatment but do not form infection threads nor nodules (Miwa et al. 2006).

A network of transcription factors (TFs) reprograms transcription downstream of LjCCaMK/ MtDMI3 activation (reviewed by Popp and Ott 2011). The symbiotic transcription factor, LjCYCLOPS, is a phosphorylation substrate of LjCCaMK. The phosphorylation of LjCYCLOPS enables it to bind to specific *cis*-elements on target gene promoters and induce gene expression. Mutations in *LjCYCLOPS* severely inhibit rhizobial infection; almost all infection threads are arrested in the initial stage (Yano et al. 2008; Singh et al. 2014; Cerri et al. 2017).

Additional components downstream of CCaMK include the GRAS proteins NODULATION SIGNALING PATHWAY1 (LjNSP1/ MtNSP1) and LjNSP2/ MtNSP2. In *ljnsp1*/ *mtnsp1* and *ljnsp2*/ *mtnsp2* mutants induction of $Ca^{2+}$ spiking is not affected, while only a low number of deformed root hairs are observed and infection threads are absent (Smit et al. 2005; Kaló et al. 2005; Heckmann et al. 2006; Murakami et al. 2006). It is unclear how LjNSP1/ MtNSP1 and LjNSP2/ MtNSP2 are activated but these proteins are critical for transmitting signals downstream of LjCCaMK/ MtDMI3 to promote the root hair response.

MtNSP1 and MtNSP2 form a heterodimer, which is required for MtNSP1 to bind to the promoter of its target genes (Hirsch et al. 2009). In a current model proposed for *M. truncatula*, IPD3 constitutes large protein complexes with NSP1 and NSP2, through interaction with DELLA proteins (Fonouni-Farde et al. 2016; Jin et al. 2016). *Lotus japonicus* CYCLOPS also interacts with DELLA1 and efficiently activates its target gene (Pimprikar et al. 2016). LjCYCLOPS/ MtIPD3, LjNSP1/ MtNSP1, and LjNSP2/ MtNSP2 are essential for activation of two other transcription factor genes, *ERF REQUIRED FOR NODULATION 1* (*LjERN1/ MtERN1*) and *NODULE INCEPTION* (*LjNIN/ MtNIN*) (Schauser et al. 1999; Marsh et al. 2007; Middleton et al. 2007; Yano et al. 2008; Singh et al. 2014; Fonouni-Farde et al. 2016; Jin et al. 2016; Cerri et al. 2017).

The transcription factor LjNIN/ MtNIN plays roles in infection thread formation, nodule primordium development, and negative feedback regulation to restrict root nodule numbers (auto-regulation of nodulation). *LjNIN/ MtNIN* expression is strongly induced by rhizobial infection. In *ljnin/ mtnin* mutants, root hairs exhibit excessive curling after infection but cannot form infection threads nor nodule primordia (Schauser et al. 1999; Marsh et al. 2007). Targets of LjNIN, such as *NODULATION PECTATE LYASE* (*LjNPL*), *SCAR-Nodulation* (*LjSCARN*), and *LjEpr3*, are involved in infection thread formation (Figure 2d). *LjNPL* encodes a pectate lyase and mediates cell wall degradation during infection thread initiation (Xie et al. 2012). LjSCARN binds to LjARPC3 and promotes formation of new actin filaments in root hairs during infection thread development (Qiu et al. 2015). *LjEpr3* is also targeted and positively regulated by LjNIN (Kawaharada et al. 2017a). Targets of LjNIN also function in nodule primordium formation and control of nodule number. Nuclear Factor-YA1 (LjNF-YA1) and LjNF-YB1 promote cortical cell division for production of nodule primordia (Soyano et al. 2013). CLE Root Signal1 (LjCLE-RS1) and LjCLE-RS2 function as root-derived mobile signals; they are transported

to the shoot and activate autoregulation of nodulation to suppress excessive production of root nodules (Okamoto et al. 2009; Soyano et al. 2014).

Although many components of the root nodule symbiosis pathway have been discovered, knowledge of the relationship and interplay among the constituent genes is still limited. For example, a number of protein complexes involving critical factors have been suggested, such as MtIPD3−MtNSP1−MtNSP2, MtNSP1−MtNSP2−MtNF-YA1, and LjNSP2−LjIPN2, but it is unclear how they are integrated for different functions (Kang et al. 2014; Laloum et al. 2014). Further studies are needed to explore the coordination of these transcription factors and to examine spatiotemporal patterns in their regulation of gene expression.
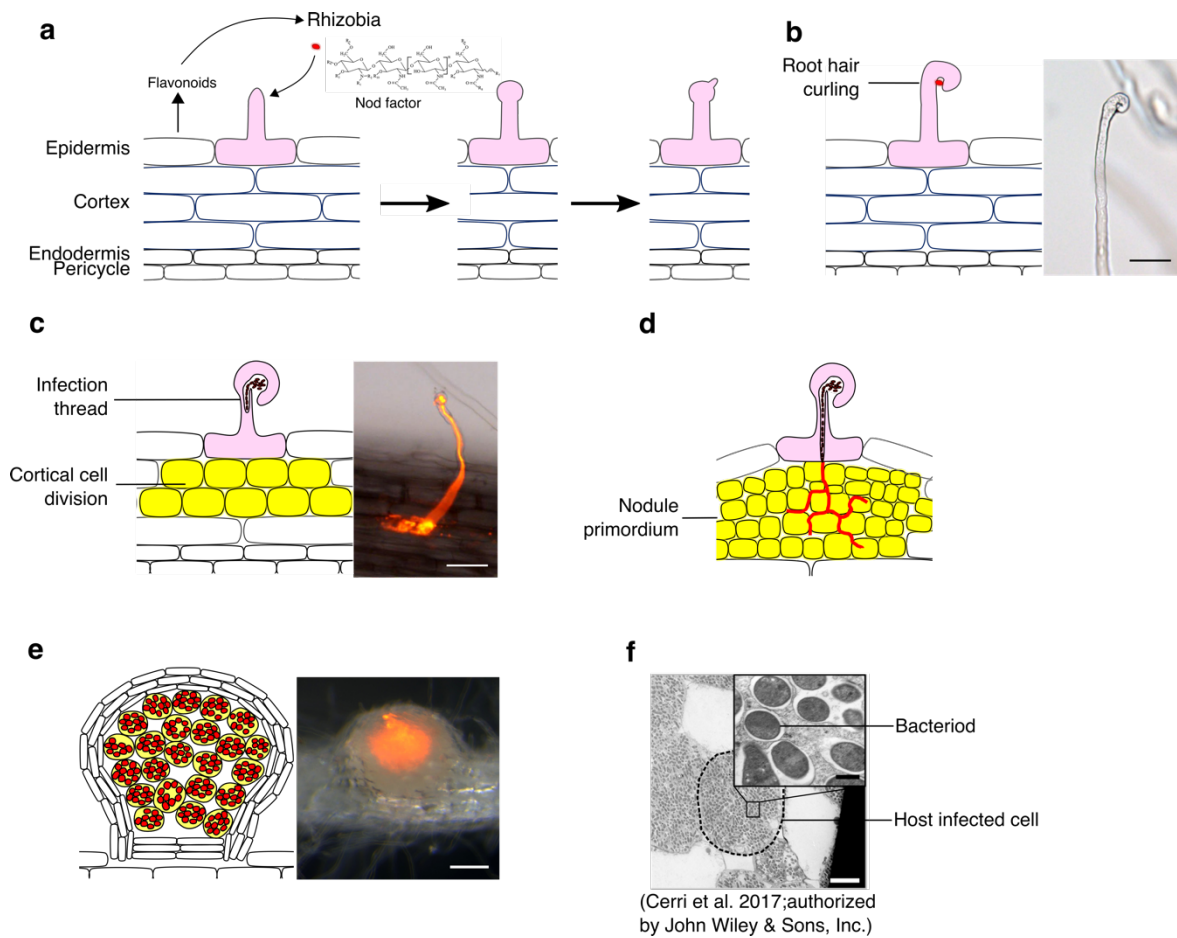
**Figure 1 Schematic illustration of root nodule formation process.**

(**a**) Rhizobia sense the flavonoids released by the host legume and synthesize Nod factors. Perception of the Nod factors by the host plant induces root hairs swelling and redirection of tip growth. (**b**) The root hair grows toward rhizobia and entraps the bacteria in a tight curl. The right panel shows a light microscopic image of a curled root hair. (**c**) Rhizobia invade the host root through infection threads, which are initiated at infection foci in the curled root hair. Infection threads grow toward the cortex. Cell division occurs underneath the infection site to form a nodule primordium. The right panel shows a root hair infected by rhizobia; the infection thread is visualized by DsRed-labeled *Mesorhizobium loti*. (**d**) Infection threads ramify within the nodule primordium. (**e**, **f**) Rhizobia enclosed in infection threads

are budded off and released into the host cells. (**f**) Electron microscopy images of a root nodule. The magnified image shows infected cells, and the boxed area shows bacteroids surrounded by a symbiosomal membrane (Cerri et al. 2017; authorized by John Wiley & Sons, Inc, license number 4653341113739).
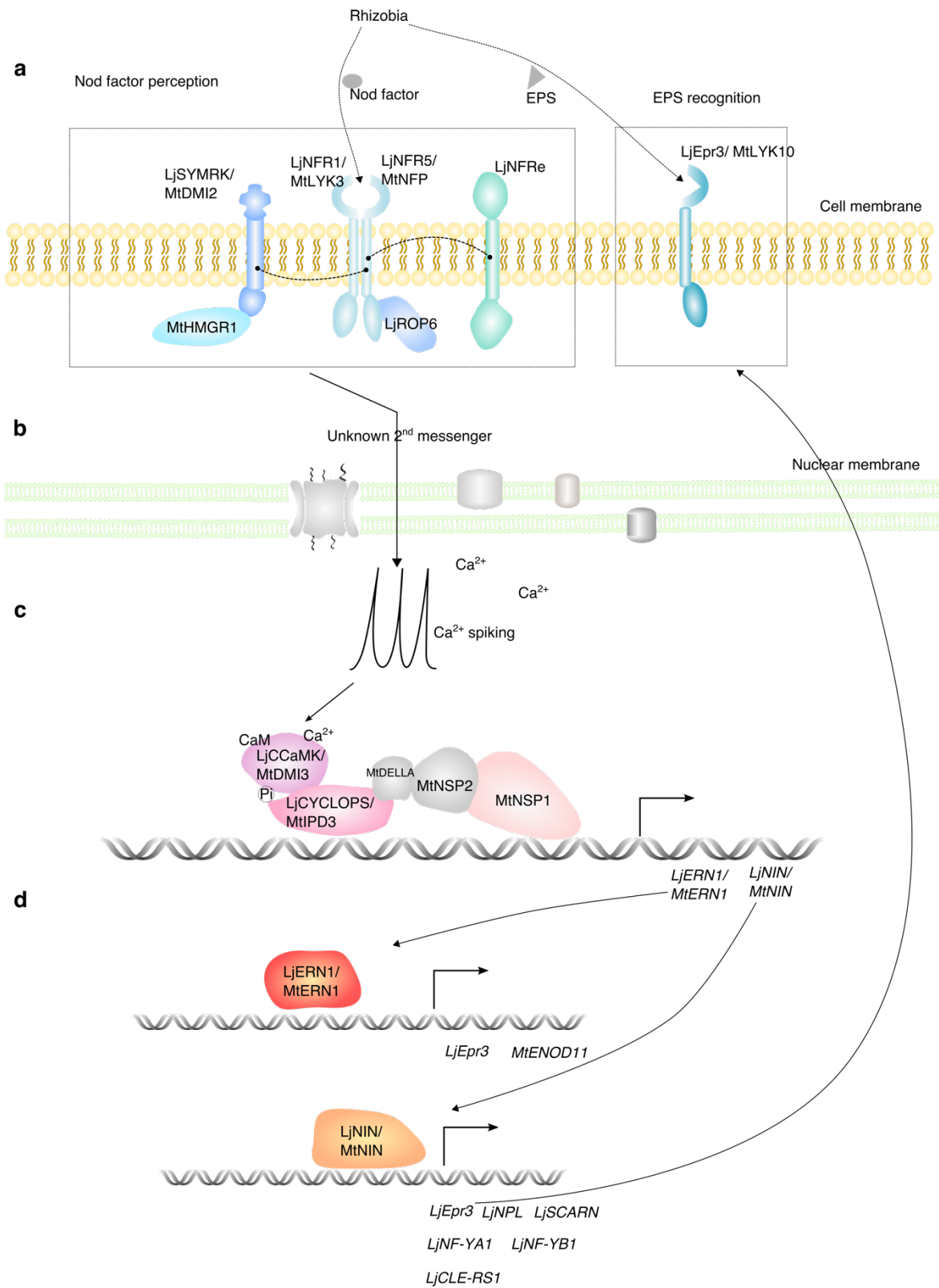
**Figure 2 Model of nodulation signaling in legumes.**

(**a**) Rhizobia are recognized by the host plant via a two-step recognition system on the cell membrane. Nod factors produced by rhizobia are recognized by the Nod factor receptors LjNFR1/ MtLYK3, LjNFR5/ MtNFP, and LjNFRe. This activates Nod factor signaling and subsequently LjEpr3, which perceives EPS released by rhizobia and facilitates rhizobia entry. LjSYMRK and LjNFRe associate with and phosphorylate LjNFR5 (dashed line). (**b**) Perception of Nod factors on the plasma membrane transmits the signal and induces $Ca^{2+}$ oscillation (spiking) in the nucleus. (**c**) The $Ca^{2+}$ spiking is decoded by LjCCaMK/ MtDMI3, which subsequently phosphorylates LjCYCLOPS/ MtIPD3. LjCYCLOPS/ MtIPD3 constitutes a protein complex with other transcription factors and activates gene expression, such as *LjERN1/ MtERN1* and *LjNIN/ MtNIN*. (**d**) LjERN1/ MtERN1 and LjNIN/ MtNIN regulate expression of downstream genes, such as *LjEpr3* (described above), *LjNPL* (involved in cell wall degradation), and *LjNF-YA1* (involved in nodule primordium formation).

# 2. INTRODUCTION

Legumes interact with nitrogen-fixing bacteria, termed rhizobia, in the soil and establish a symbiotic relationship. Host legumes undergo *de novo* organogenesis and form root nodules, which are inhabited by rhizobia. In the model legumes *L. japonicus* and *M. truncatula*, rhizobia infect the host through root hairs. In wild-type plants, rhizobial infection induces root hair swelling and re-initiation of polar growth to cause tight curling of the root hairs. Rhizobia are entrapped in the infection pocket and then invade the epidermis through the infection thread, a tip-growing tubular structure. Molecular genetic studies have identified numerous genes involved in infection thread formation. The infection signal triggers the $Ca^{2+}$ oscillation in the nucleus. A protein kinase, CCaMK (from this paragraph, the name of genes and proteins in *L. japonicus* are primarily used unless otherwise specified), acts as a decoder of the $Ca^{2+}$ signal and phosphorylates the transcription factor CYCLOPS, which directly activates the expression of *ERN1* and *NIN* (Singh et al. 2014; Cerri et al. 2017).

Previously, collaborator and I characterized two allelic symbiotic mutant lines, *ern1-5* and *ern1-6*. Similar to *M. truncatula ern1* mutants, *L. japonicus ern1-5* and *ern1-6* mutants show severe infection thread deficiency (Middleton et al. 2007; Yano et al. 2017). *ern1* mutants undergo root hair deformation upon rhizobial infection but rarely form curled root hairs. Many root hairs in *ern1* display a balloon-shaped tip, which may interfere with rhizobial colonization (Cerri et al. 2016; Yano et al. 2017). *ern1* mutants occasionally produce mature root nodules; however, microscopic observation revealed that transcellular infection threads are absent from these nodules and rhizobia probably colonize the cell via crack entry or alternative means (Cerri et al. 2017; Kawaharada et al. 2017b). These phenotypes of *ern1* mutants suggest that ERN1 functions in root hair curling and infection thread formation.

ERN1 is a transcription factor belonging to AP2/ERF family. To date, two genes have been shown to be regulated by ERN1, namely *ENOD11* in *M. truncatula* and *Epr3* in *L. japonicus*. MtERN1 and the NSP1−NSP2 heterodimer bind to different sites on the *ENOD11* promoter and coordinately regulate *ENOD11* expression in response to Nod factors and rhizobial infection (Andriankaja et al. 2007; Cerri et al. 2012). *Lotus japonicus* ERN1 binds to the *Epr3* promoter *in vitro* and activates its promoter in a transient assay using *Nicotiana benthamiana* leaves. Expression of *proEpr3:GUS* is detected in the epidermis of *L. japonicus* roots after rhizobial infection. This expression is diminished by loss-of-function mutation of ERN1 (Kawaharada et al. 2017a; Kawaharada et al. 2017b). ENOD11 and Epr3 participate in cell wall modification and rhizobial recognition, respectively. The function of these ERN1 targets suggests an association of ERN1 with early infection events.

The spatiotemporal expression patterns of *ERN1* show correlation with infection thread formation. Expression analysis using *proERN1:GUS* showed strong GUS signal in infected root hairs, resulting in a patchy expression pattern in the root epidermis (Middleton et al. 2007; Cerri et al. 2017; Yano et al. 2017). Transcriptome analysis conducted on *M. truncatula* root hairs and quantitative real-time PCR (qRT-PCR) analysis in *L. japonicus* showed that *ERN1* expression increases within 12 hours after infection, which corresponds to the stage of root hair deformation (Larrainzar et al. 2015; Yano et al. 2017). These expression patterns of ERN1 suggest the involvement of this factor in the early response of the root hair during rhizobial infection.

ERN1 also plays a role in nodule primordium formation. Cytokinin promotes cortical cell division during nodule development and exogenous application of $10^{-8}$ M 6-benzylaminopurine (6-BA) induces spontaneous nodules in *L. japonicus* roots (Hechmann et al. 2011). *ERN1* expression is induced by cytokinin application. This up-regulation of

*ERN1* was reduced in mutants of the cytokinin receptor *CRE1* in *M. truncatula*, suggesting that ERN1 is involved downstream of cytokinin signaling (Plet et al. 2011). Exogenous application of cytokinin does not induce formation of spontaneous nodules in the *L. japonicus ern1* mutant (Kawaharada et al. 2017b), indicating that ERN1 is necessary for cytokinin-induced cell division in *L. japonicus*. Nevertheless, *ern1* mutants are able to produce nodule primordia and mature root nodules. The exact function of ERN1 in cytokinin-induced formation of nodule primordia is unclear.

Studies on *L. japonicus* have demonstrated the transcriptional hierarchy of CYCLOPS−NIN and CYCLOPS−ERN1. However, mutants of these three factors showed variation in phenotypes involving root hair shape, infection thread formation, and nodule primordium formation. In roots of *cyclops* mutant, rhizobia are trapped in curled root hairs but infection threads are not initiated. Nodule primordia develop but nodule cells are not colonized by the bacteria. *ern1* mutants show swollen root hairs and decreased number of infection threads but are able to form mature root nodules. *nin* mutants exhibit excessively curled root hairs but all infections are arrested as micro-colonies. *nin* mutants fail to develop nodule primordia. The differences in phenotypes suggest that CYCLOPS, ERN1, and NIN have a more complicated relationship than a simple linear transcription hierarchy in the signaling pathway. In particular, the relationship of ERN1 with NIN remains unclear. A gene network analysis was conducted on *M. truncatula* based on transcriptome data for root hairs (Liu et al. 2019). This analysis showed that ERN1 and NIN function in two parallel regulons. However, *NIN* expression is increased in the *ern1* single and *ern1 ern2* double mutants (Cerri et al. 2016; Liu et al. 2019). Expression of *ERN1* and its paralog, *ERN2*, is also up-regulated in *M. truncatula nin* mutants (Liu et al. 2019). Thus, expression of *ERN1* and *NIN* seems to be influenced by each other during infection processes in the root epidermis of *M. truncatula*. On the other hand, in *L. japonicus*, loss-of-function of *NIN* does

not significantly increase the *ERN1* expression level (Yano et al. 2017), and the *ern1* mutation reduces the expression level of *NF-YA1*, which is a direct target of NIN (Soyano et al. 2013; Kawaharada et al. 2017b). Therefore, ERN1 may positively regulate *NIN* expression in *L. japonicus*.

The aim of this study was to gain a better understanding of how ERN1 and NIN integrate their functions with CYCLOPS in the root nodule symbiosis signaling pathway. Here, I investigated the effect of *ERN1* on *NIN* expression in *L. japonicus* and their genetic relationship during infection thread development. I demonstrate that *ERN1* contributes to *NIN* expression in a CYCLOPS-independent manner. Moreover, ectopic expression of *ERN1* or *NIN* suppressed the infection thread deficiency of the *cyclops-3* mutant. However, *ERN1* and *NIN* failed to rescue the defective development of infection threads in the *nin-2* and *ern1-1* mutants, respectively. I propose that ERN1 and CYCLOPS play both overlapping and distinct roles in regulation of symbiotic epidermal responses and *NIN* expression in *L. japonicus*.

# 3. RESULTS

## 3.1 The *ern1* mutation reduces *NIN* expression in response to rhizobial infection

The *L. japonicus ern1* and *nin* mutants show severe infection thread deficiency and reduced expression of root nodule symbiotic genes including *Epr3* and *NF-YA1* (Schauser et al. 1999; Cerri et al. 2017; Kawaharada et al. 2017a; Kawaharada et al. 2017b), indicating that ERN1 and NIN play essential roles in the signaling pathway regulating infection thread formation. Although *ERN1* and *NIN* have been shown to be direct targets of CYCLOPS in *L. japonicus*, the relationship between these transcription factors during nodulation has not yet been fully elucidated (Singh et al. 2014; Cerri et al. 2017). To assess the interplay between these transcription factors, I conducted qRT-PCR analysis in *L. japonicus* plants of the wild-type accession Gifu B-129 and the *ern1-1* mutant (*LORE1* line 30034615) using *Ubiqutin* gene as a reference. The *LORE1* retrotransposon element in *ERN1* is present at the coding region corresponding to the AP2-DNA binding domain in the *ern1-1*. I found that *NIN* expression was distinctly affected in *ern1-1* roots inoculated with *Mesorhizobium loti* (Figure 3a). In wild-type roots, *NIN* transcript levels increased over 20-fold at 1 and 3 days post inoculation (dpi), whereas the levels decreased to less than one-third of the wild type in *ern1-1* mutants. I further examined *NIN* expression in *ern1-5* and *ern1-6*, *ern1* alleles in the Miyakojima MG-20 background (Yano et al. 2017), to verify this expression pattern. This reduction of *NIN* expression was reproduced in these *ern1* allelic mutants, using two reference genes, *Ubiquitin* and *ATP synthase* (Figure 3b, d). These results indicate that *ERN1* is required for *NIN* expression in response to rhizobial infection in *L. japonicus*.

The reduction of the infection-induced *NIN* expression in *ern1-1* is reminiscent of that in *cyclops-3* mutants (Yano et al. 2008). The *cyclops-3* mutation caused a significant decline in *NIN* expression at 1 and 3 dpi (Figure 3a). However, the expression level of this

gene was still higher in inoculated *cyclops-3* roots than in uninoculated ones, suggesting that factors other than CYCLOPS are involved in *NIN* expression regulation. To determine whether *CYCLOPS* and *ERN1* play independent roles in regulating *NIN* expression, I generated a *cyclops-3 ern1-1* double mutant and found that *NIN* expression levels at 1 and 3 dpi were further reduced compared to the single mutants, and were not up-regulated comparing to double mutant itself at 0 dpi. Lower *NIN* expression levels in *ern1-1* and *cyclos-3 ern1-1* were confirmed by second reference gene, *ATP synthase* (Figure 3c). I then measured the expression of *NF-YA1*, *NPL*, and *CLE-RS1*−three direct targets of NIN (Xie et al. 2012; Soyano et al. 2013; Soyano et al. 2014)−and observed that each gene showed lower expression levels in *cyclops-3*, *ern1-1*, and double mutants compared with those of the wild type (Figure 4). The findings verified that *NIN* expression was affected by *cyclops* and *ern1* mutation. These results indicate that *ERN1* and *CYCLOPS* are coordinately involved in regulating *NIN* expression.

NIN regulates nodule organogenesis as well as infection thread development. Cytokinin induces *NIN* expression and promotes cortical cell division to facilitate nodule primordium development (Murray et al. 2007; Soyano et al. 2013). *ERN1* is also involved in cytokinin-induced cortical cell division (Kawaharada et al. 2017b). Its expression is up-regulated by exposure to cytokinin in *M. truncatula* (Plet et al. 2011; van Zeijl et al. 2015). To further examine if the *ern1-1* mutation affects cytokinin-induced *NIN* expression in *L. japonicus*, I treated seedlings with 10 nM of the cytokinin, 6-BA (Figure 5). This concentration of 6-BA efficiently induces pseudo-nodule formation and has only minor effects on root development (Heckmann et al. 2011). In wild-type roots, *NIN* expression rapidly increased to a level approximately 40-fold that of the control within 3 hours of treatment and declined by half after 24 hours of treatment. In *cyclops-3*, the expression pattern of *NIN* was similar to that of the wild type. By contrast, in *ern1-1* and *cyclops-3*

*ern1-1*, *NIN* expression levels were approximately half of the wild type at the 3-hour time point. However, 24 hours after treatment, the *NIN* expression levels of these mutants were indistinguishable from those of the wild type and *cyclops-3*. Thus, *ERN1* positively influenced *NIN* expression only at the early time point after cytokinin treatment. Taken together, these results indicate that *ERN1* is involved in regulating *NIN* expression in addition to *CYCLOPS*. Since *ern1* mutations affected *NIN* expression at early stages of infection and both *ERN1* and *NIN* expressed in infected root hairs (Figure 6a, b; Cerri et al. 2017; Kawaharada et al. 2017b; Yano et al. 2017), I focused on responses of root hairs upon rhizobial infection in further experiments.

## 3.2 The *cyclops-3 ern1-1* double mutant shows severe symbiotic phenotypes

The *NIN* expression levels in *ern1-1* and *cyclops-3 ern1-1* indicate that *ERN1* influences *NIN* expression at early infection stages. To investigate whether *ERN1* affects infection thread formation coordinately with *CYCLOPS*, I characterized the symbiotic phenotypes of *cyclops-3 ern1-1* plants (Figure 7). I inoculated *L. japonicus* seedlings with *M. loli* constitutively expressing *DsRed* to visualize their infection status. By 14 dpi, 85% of nodules formed in wild-type roots have pink color due to expression of leghemoglobin, indicating that most of them were mature nodules (Figure 7a, e; Ott et al., 2005). By contrast, 100% and 79% of nodules formed in *cyclops-3* and *ern1-1* mutants remained immature (Figure 7b, c, f, g, i; Yano et al. 2008; Cerri et al. 2017; Kawaharada et al. 2017b; Yano et al. 2017). Rhizobia multiplied in the infection chamber of the curled root hair, forming micro-colonies, followed by infection thread development. Over 100 infection threads were produced (Figure 7j), and a small population of infection events at the micro-colony stage was present in wild-type roots at this time point (Figure 7k). On the other hand, formation of infection threads was inhibited in *cyclops-3* and *ern1-1* roots as reported previously

(Figure 7j; Yano et al. 2008 and 2017; Kawaharada et al. 2017b; Cerri et al. 2017). Mean numbers of infection threads in *cyclops-3* and *ern1-1* were 0 and 0.8 per plants, respectively. Micro-colony numbers were increased in *cyclops-3* roots compared with wild-type roots (Figure 7k), although total numbers of infection events (formation of infection threads and micro-colonies) were still higher in wild-type roots. This result implies the arrest of infection processes after entrapment of rhizobia in *cyclops-3* mutants (Yano et al. 2008). The *ern1-1* phenotype was milder than that of *cyclops-3* mutants in regard to infection thread formation. However, total numbers of infection events visualized by DeRed in *ern1-1* roots (8 per plants) were less than that of wild type and *cyclops-3* mutants (119 and 16 per plants, respectively). The *ern1-1* phenotype contains aspects different from that of *cyclops-3* mutants. Nevertheless, the *cyclops-3* and *ern1-1* mutants displayed infection events that appeared as short infection threads and micro-colonies, as detected by DsRed fluorescence. *cyclops-3 ern1-1* double mutants−similarly to *cyclops-3*−formed no infection threads, but micro-colony numbers were less than those of *ern1-1* mutants (Figure 7j, k). In addition, no nodule and nodule primordia were observed in double mutants at 14 dpi (Figure 7d, h, i). Therefore, the *ern1-1* and *cyclops-3* mutations additively or synergistically affect the formation of infection thread and nodule primordia.

Root hair deformation is a critical step for the entrapment of rhizobia. Rhizobial infection elicits morphological changes to root hairs, such as curling and branching (Fisher and Long, 1992). Therefore, I observed root hair morphologies at 5 dpi to investigate whether the severe deficiency in infection of *cyclops-3 ern1-1* is caused by incorrect root hair deformation. I categorized the shapes of root hairs in mock-treated or inoculated wild-type and mutant roots into five major types: curled (shepherd's crook), branched, excessively curled, swollen, and waved structures (Figure 8). These morphological groups were defined by two independent preliminary observations and comparison between mock-

treated and inoculated roots. Although root hairs exhibiting these structures were observed in the absence of rhizobia, numbers of these root hairs were either not significantly different among wild-type and mutant roots or not increased in certain genetic backgrounds in response to inoculation with rhizobia (Figure 8a–j).

The curled tip of the root hair was the dominant (and typical) morphological phenotype of wild-type roots inoculated with *M. loti* (Figure 8a, b). By contrast, fewer curled root hairs developed in the *cyclops-3*, *ern1-1*, and *cyclops-3 ern1-1* mutants. Instead, branched root hairs were commonly observed in inoculated *cyclops-3* and *ern1-1* roots (Figure 8c, d). In addition, *cyclops-3* and *ern1-1* displayed characteristic root hair morphologies, namely excessively curled root hairs in *cyclops-3* (Figure 8e, f) and balloon-shaped (swollen) root hairs in *ern1-1* (Figure 8g, h; Yano et al. 2017). Thus, variation in the root hair structure of inoculated *cyclops-3* and *ern1-1* roots was observed. Unlike the *cyclops-3* and *ern1-1* single mutants, only a few root hairs in the *cyclops-3 ern1-1* double mutant exhibited curled and branched structures (Figure 8b, d). Rhizobia are usually entrapped by curled root hair tips and narrow slits between branched root hair tips. Less micro-colonies in the double mutants probably reflected fewer root hairs exhibiting these morphological phenotypes. Waved root hairs were predominantly observed in the double mutants (Figure 8i, j). This phenotype was occasionally observed in wild-type, *cyclops-3*, and *ern1-1* roots inoculated with rhizobia, but the frequency was not significantly different from that of mock-treated roots. The total number of deformed root hairs in *cyclops-3 ern1-1* was half that of the single mutants (Figure 8k). These results suggested that *cyclops-3 ern1-1* roots were either less sensitive to rhizobial infection than wild-type roots or defective in the early stages of the root hair response to infection.

## 3.3 ERN1 increases *NIN* expression level in an infection-dependent manner

Since *ERN1* is required for efficient *NIN* expression in *L. japonicus*, I reasoned that *ERN1* would induce *NIN* expression *in planta*. To explore this possibility, I overexpressed *ERN1* from *L. japonicus Ubiquitin* promoter in *ern1-1* hairy roots to remove effects of endogenous *ERN1*. At the beginning, I compared *NIN* expression levels between roots overexpressing *ERN1* and those transformed with an empty vector in the absence of rhizobia. However, *ERN1* overexpression did not influence *NIN* transcript levels (Figure 9a). To confirm the *ERN1* construct is functional, roots overexpressing *ERN1* was inoculated with *M. loti*. *NIN* transcript levels were increased in roots overexpressing *ERN1* after inoculation, while it was not significantly changed in the empty vector controls. This result indicates that *ERN1* overexpression alone is not sufficient for up-regulation of *NIN* expression, as rhizobial infection was required for the accumulation of its transcript. To evaluate whether CYCLOPS is involved in this induction of *NIN* expression, I overexpressed *ERN1* in *cyclops-3 ern1-1* roots. *ERN1* overexpression still increased *NIN* expression levels in the double mutant in the presence of rhizobia (Figure 9b). At 1 dpi, *NIN* was expressed at lower levels in *cyclops-3 ern1-1* compared to *ern1-1* roots, but its expression level was restored to that detected in *ern1-1* at 3 dpi. Thus, CYCLOPS is dispensable for increasing *NIN* transcript levels in roots overexpressing *ERN1*. To validate this ERN1-dependent gene expression profile, I examined the expression of *CLE-RS1* and *NF-YA1*, direct targets of NIN (Soyano et al. 2013 and 2014), and *Epr3*, whose promoter is targeted by both ERN1 and NIN (Kawaharada et al. 2017a). These genes are expressed in infected root hairs (Figure 6c; Kawaharada et al. 2015 and 2017a). Like *NIN*, expression of these genes was significantly induced upon rhizobial infection in roots overexpressing *ERN1*, even in the double mutant (Figure 10a, b, g, h, m, n). Hence, *ERN1* overexpression leads to induction of *NIN* expression in the absence of CYCLOPS depending on rhizobial infection.

In addition to *NIN*, the expression levels of *NF-YA1*, *CLE-RS1*, and *Epr3* were increased by *ERN1* overexpression upon infection in *ern1-1* and *cyclops-3 ern1-1*. To determine whether expression of *NF-YA1*, *CLE-RS1*, and *Epr3* was increased by the indirect effect of elevated *NIN* expression or direct activation by ERN1, I repeated the *ERN1* overexpression experiment in *nin-2* mutants (Figure 10c, i, o). The expression levels of *NF-YA1*, *CLE-RS1*, and *Epr3* were not significantly increased by *ERN1* overexpression, even with rhizobial infection. These observations indicated that *NF-YA1*, *CLE-RS1*, and *Epr3* were up-regulated in *ern1-1* and *cyclops-3 ern1-3* as a secondary effect of NIN rather than as a direct influence of ERN1.

Next, I examined whether Nod factor signaling is necessary for ERN1-dependent induction of *NIN* expression. I made use of the *nfr1-3* and *ccamk-3* mutants, which are defective in Nod factor perception and decoding of the $Ca^{2+}$ signals induced by Nod factor signaling, respectively (Radutoiu et al. 2003; Tirichine et al. 2006). In addition to these factors, I examined the requirement of *NSP1* for the effect of *ERN1* overexpression, since this transcription factor is essential for *NIN* expression in response to rhizobial infection and involved in symbiotic root hair responses downstream of CCaMK activation (Marsh et al. 2007; Hayashi et al. 2010; Madsen et al. 2010). Although *NIN* transcript levels were slightly up-regulated in *nfr1-3* and *ccamk-3* roots overexpressing *ERN1* (Figure 9c, d), its expression level did not significantly increase even after inoculation with rhizobia. *NIN* expression levels in *nsp1-1* roots constitutively expressing *ERN1* did not significantly differ from those of the empty vector controls in the absence or presence of rhizobia (Figure 9e). In line with *NIN* expression, no significant differences in the expression levels of *NF-YA1, CLE-RS1*, and *Epr3* were detected among the *nfr1-3*, *ccamk-3*, and *nsp1-1* mutants (Figure 10d−f, j−l, p−r). Thus, Nod factor signaling and *NSP1* are crucial for the effect of *ERN1* on expression of *NIN* and its target genes.

## 3.4 Ectopic expression of *ERN1* and *NIN* promotes infection thread formation in *cyclops-3*

The direct binding of CYCLOPS to specific *cis*-elements in the *ERN1* and *NIN* promoters has been demonstrated at the molecular level (Singh et al. 2014; Cerri et al. 2017). Our findings suggest that ERN1 also positively influence *NIN* expression. To investigate how the interplay between these transcription factors influences infection thread formation, I conducted a series of functional complementation studies by generating hairy roots from the *cyclops-3*, *ern1-1*, and *nin-2* mutants (Figure 11). Constitutive expression of *CYCLOPS* driven by the *Ubiquitin* promoter restored infection thread formation on *cyclops-3* roots (Figure 11c, o) but did not increase the number of infection threads on *ern1-1* (Figure 11g, p) or *nin-2* roots (Figure 11k, q), indicating that ERN1 and NIN are required for infection thread formation downstream or in parallel with CYCLOPS. By contrast, *ERN1* expression driven by the *Ubiquitin* promoter suppressed the infection thread-defectiveness of the *cyclops-3* and *ern1-1* mutants (Figure 11d, h, o, p) but did not lead to infection thread formation in the *nin-2* mutant (Figure 11l, q). Thus, ERN1 is capable of functionally replacing CYCLOPS to induce infection thread production but requires *NIN* for infection thread initiation. These results are consistent with the transcriptional hierarchy identified in this and previous studies.

Finally, I assessed the functional relationship of *NIN* with other genes during infection thread development. As *NIN* overexpression inhibits nodulation (Soyano et al. 2014), I ectopically expressed *NIN* under the control of the *CYCLOPS* promoter. *nin-2* transformed with *proCYCLOPS:NIN* generated infection threads on root epidermis (Figure 11m, q). *NIN* expression driven by the *CYCLOPS* promoter recovered infection thread formation in *cyclops-3* roots (Figure 11e, o). This result indicates that NIN is sufficient to

confer infection threads in *cyclops-3* mutants and is consistent with the idea that *NIN* is downstream of CYCLOPS. However, the same construct failed to suppress the infection thread-deficient phenotype of *ern1-1* mutants (Figure 11i, p). These results suggest that although NIN is a critical factor downstream of ERN1, to promote infection thread development, NIN may require ERN1 or genes downstream of ERN1.

## 3.5 A subset of genes downstream of ERN1 were NIN-dependent

To gain insight into the function of ERN1 in promoting infection thread formation, I conducted transcriptome analysis (RNA-seq) to profile gene expression in *ern1-6* mutants. *L. japonicus* wild-type MG-20 and *ern1-6* (Yano et al. 2017) were inoculated with *M. loti* MAFF303099. Three biological replicates were used for sequencing with each consisting of 20 plants. The characterization of *cyclops-3 ern1-1* root hair shape suggested that ERN1 may regulate root hair deformation and infection thread formation. Rhizobia induce root hair deformation within hours after inoculation. Preliminary observations confirmed that at 1 dpi, root hairs were deformed but infection threads were not yet formed. To reveal the transcriptional change in *ern1* corresponding to the stage of root hair deformation, I focused on transcriptional changes at 1 dpi. Principal component analysis (PCA) demonstrated separation of the wild-type and *ern1-6* samples collected at 0 and 1 dpi (Figure 12a). In total, 2554 genes were up-regulated and 1218 genes were down-regulated in wild-type roots in response to rhizobial inoculation (Figure 12b; fold change > 1.5, FDR < 0.1). At 1 dpi, 1380 genes were differentially expressed in *ern1-6* compared with the wild type (820 down- and 560 up-regulated). Among the 2554 inoculation-induced differentially expressed genes (DEGs), 260 genes showed decreased transcript levels in *ern1-6* at 1 dpi. Only 32 of 1218 infection-repressed DEGs were up-regulated in *ern1-6*. The majority of these 32 genes were annotated without a clear function; therefore, I subsequently focused on the 260 genes for

which expression was induced by rhizobial inoculation in the wild type but reduced in *ern1-6*.

The 260 genes included several NIN targets, such as *NF-YA1* and *NPL*. To investigate if ERN1 and NIN share additional downstream genes in common, I compared the transcription profile of *ern1-6* obtained in the present RNA-seq analysis with *nin-2* transcriptome data in the *Lotus japonicus* Gene Expression Atlas (Lotus Base; Mun et al. 2016). The Gene Expression Atlas data were collected from the Gifu ecotype and were based on GeneChip analysis. To assess if genes from the Gene Expression Atlas and the RNA-seq dataset were comparable, I searched for infection-induced genes in the Gene Expression Atlas and obtained 4893 genes in total. Among the 2554 inoculation-induced genes in the RNA-seq dataset, 1566 genes were located in the Gene Expression Atlas. Cross comparison of the two datasets yielded 791 genes that showed an increased expression level after infection, although the fold changes in the Gene Expression Atlas were generally lower than those in the RNA-seq dataset (Figure 13a). I then compared the transcript levels of eight representative symbiosis genes in both datasets (Figure 13b). Although the number of fold changes differed, the transcript levels of all eight genes were increased at 1 dpi in both datasets. In brief, 791 genes exhibited similar expression patterns in the two datasets and were used for the following analyses.

Among 791 infection-induced genes, 251 were NIN-dependent, i.e. their expression in *nin-2* was reduced compared with that of the wild type (Gifu; Figure 13c) and 166 were ERN1-dependent. In total, 76 genes were dependent on both ERN1 and NIN, indicating significant overlap in genes regulated by ERN1 and NIN. Several known symbiotic genes were included in this overlapping subset, such as *APN1*, *Epr3*, and *NF-YA1*. (Table 1). This result is consistent with the decreased expression level of *NIN* in *ern1-6* (Figure 3). ERN1

influences the expression of a notable number of NIN targets, suggesting the involvement of both factors in regulating certain genes.

## 3.6 Three candidate genes as potential targets of ERN1

The comparison of the RNA-seq data and Gene Expression Atlas revealed that expression of 90 genes was dependent on ERN1 but independent of NIN. These included genes associated with auxin signaling, cell wall, cytokinin signaling, defense response, metabolism, protein binding, transcription, transporters, and other processes (Table 2). These genes may be involved in the parallel functions of ERN1 with NIN that was suggested by the functional complementation analysis. As *ern1* mutants show swollen root hairs that were not observed in nin mutants, the parallel function of ERN1 may be associated with re-initiation of root hair growth after depolarization. Three genes, namely *β-Expansin gene 2* (*EXPB2*), *Formin Homolog 8* (*FH8*), and *Rho GTPase guanine nucleotide exchange factor 3* (*RopGEF3*), have been reported to be involved in root hair growth in *Glycine max*, *Arabidopsis*, and *M. truncatula*. These genes are possible candidates that regulate root hair deformation downstream of ERN1. Expression of these genes was induced after rhizobial inoculation in wild-type and *nin-2* plants, but not in *ern1* mutants (Figure 14).
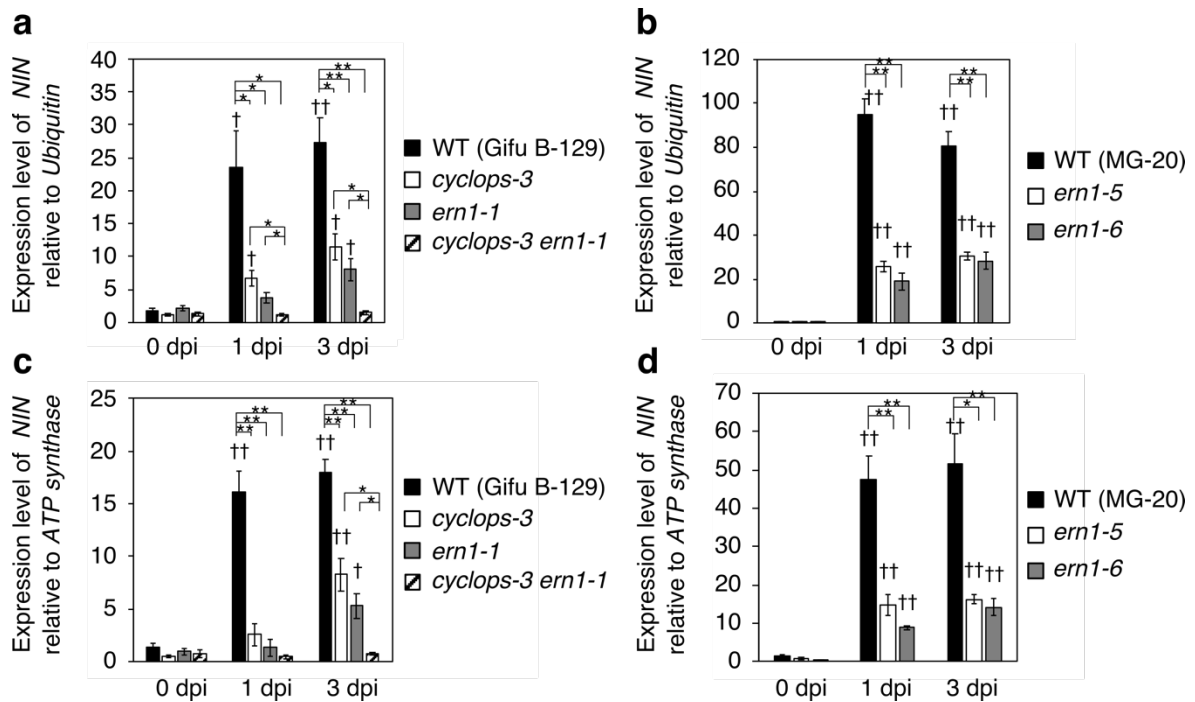
**Figure 3 qRT-PCR analysis of *NIN* expression in *L. japonicus* roots inoculated with *M. loti* MAFF303099.**

(**a**, **c**) Comparison of *NIN* expression levels in WT (Gifu B-129), *cyclops-3*, *ern1-1*, and *cyclops-3 ern1-1* mutants. (**b**, **d**) Establishment of *NIN* expression levels in different ecotype backgrounds, using WT (Miyakojima MG-20), *ern1-5*, and *ern1-6* roots. Relative expression levels were normalized to either *Ubiquitin* (**a**, **b**) or *ATP synthase* (**c**, **d**). Total RNA was extracted from whole roots harvested at the indicated time points. Data are the average fold change ± SE ($n = 3$, sample size = 16 plants). Statistical analysis was performed using Student's *t*-test (†, $P < 0.05$; ††, $P < 0.01$; compared with the 0 dpi sample. *, $P < 0.05$; **, $P < 0.01$; compared with the WT or double mutants at the indicated time point).
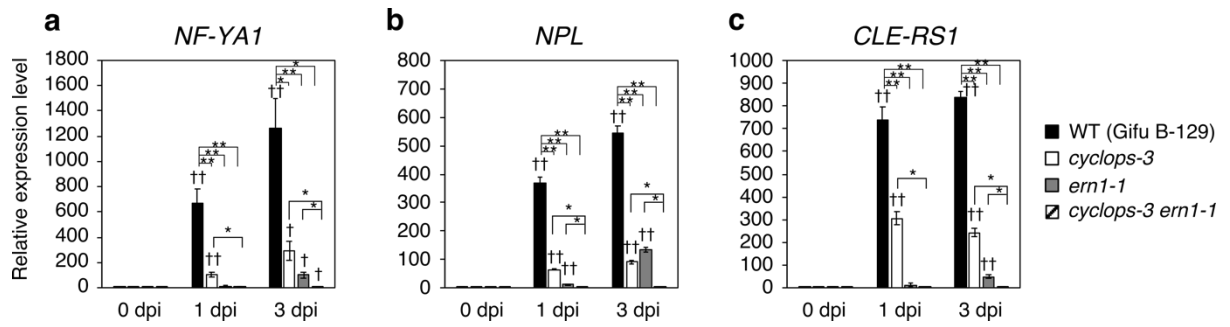
**Figure 4 qRT-PCR analysis of NIN targeting gene expression in roots inoculated with**

***M. loti* MAFF303099.**

Expression levels of *NF-YA1* (**a**), *NPL* (**b**), and *CLE-RS1* (**c**) were measured in WT (Gifu B-129), *cyclops-3*, *ern1-1*, and *cyclops-3 ern1-1*. qRT-PCR analyses were conducted using the same RNA samples as in Figure 4. Statistical analysis was performed using *t*-test as elucidated in Figure 3.
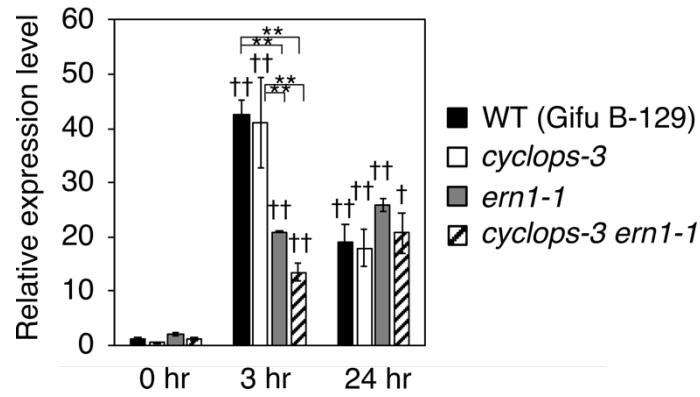
**Figure 5 qRT-PCR analysis of *NIN* expression in roots of 6-BA-treated seedlings.**

Seedlings of WT (Gifu B-129), *cyclops-3*, *ern1-1*, and *cyclops-3 ern1-1* were treated with 10 nM 6-BA. Total RNA was extracted from whole roots harvested at the indicated time points. *Ubiquitin* was used as a reference gene. Data are the average fold change ± SE ($n = 3$, sample size = 16 plants). Statistical analysis was performed using Student's *t*-test (†, $P < 0.05$; ††, $P < 0.01$; compared with the 0 dpi sample. *, $P < 0.05$; **, $P < 0.01$; compared with the WT or double mutants at the indicated time point).
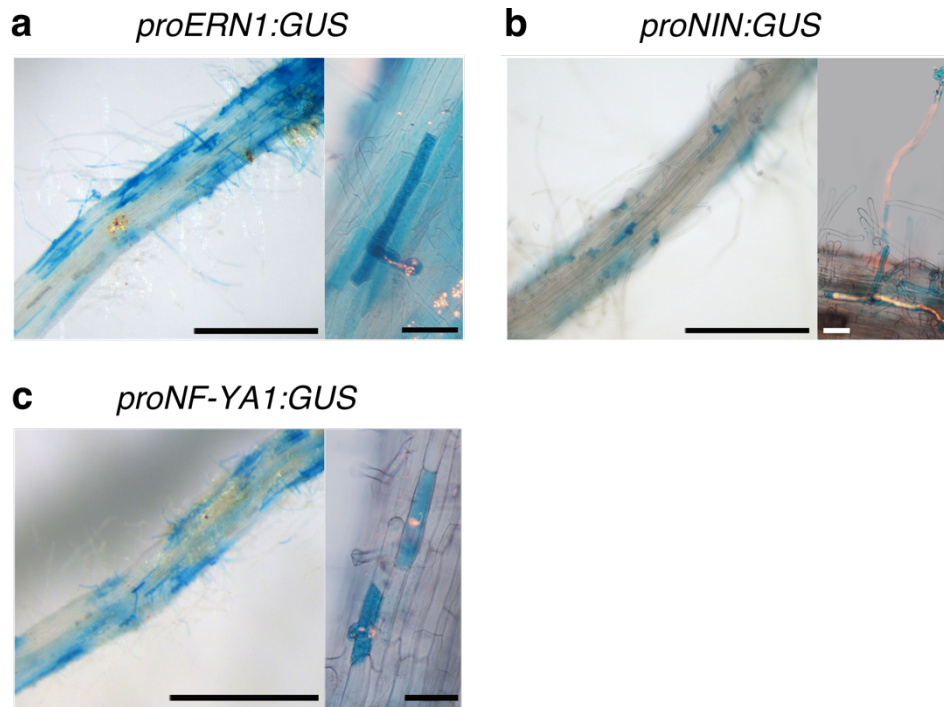
**Figure 6 GUS expression in infected root hairs.**

WT (Gifu B-129) roots were transformed with *proERN1:GUS* (**a**), *proNIN:GUS* (**b**), or *proNF-YA1:GUS* (**c**). Plants had been inoculated with DsRed-labeled *M. loti* for 3 days. Each right panel is a magnified image of infected root hairs. Images merged with DsRed fluorescence are shown. Scale bars: 0.5 mm (left panel), 50 μm (right panel).
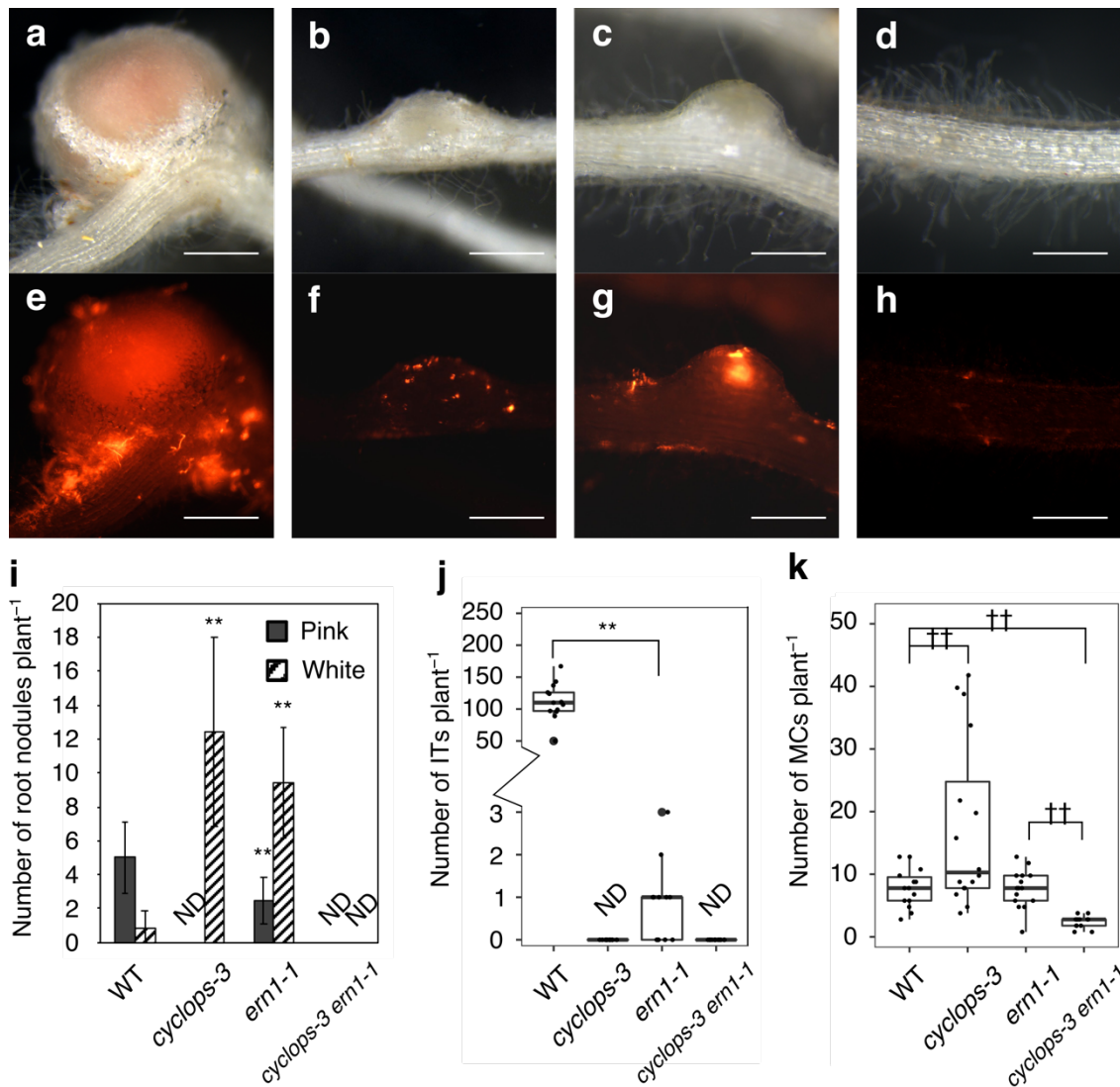
**Figure 7 Symbiotic phenotype of the *cyclops-3 ern1-1* double mutant.**

(**a**–**h**) Representative images of root nodules on the roots of the WT (Gifu B-129; **a**, **e**), *cyclops-3* (**b**, **f**), *ern1-1* (**c**, **g**), and *cyclops-3 ern1-1* (**d**, **h**). Images of bright-filed (**a**−**d**) and DsRed fluorescence (**e**−**h**) are shown. Scale bar = 500 μm. (**i**–**k**) Number of root nodules (**i**), infection threads (ITs; **j**) and micro-colonies (MCs; **k**) were quantified using 12 plants at 14 dpi. Error bars in (**i**) indicate SD. Small dots in the boxplots represent individual data points; large dots are outliers. Significance of comparison in (**i**) and (**j**) with corresponding WT control was determined by Student's *t*-test (**, $P < 0.01$). *P*-value as determined by Mann−Whitney *U* test in (**k**) are indicated by †† $P < 0.01$.
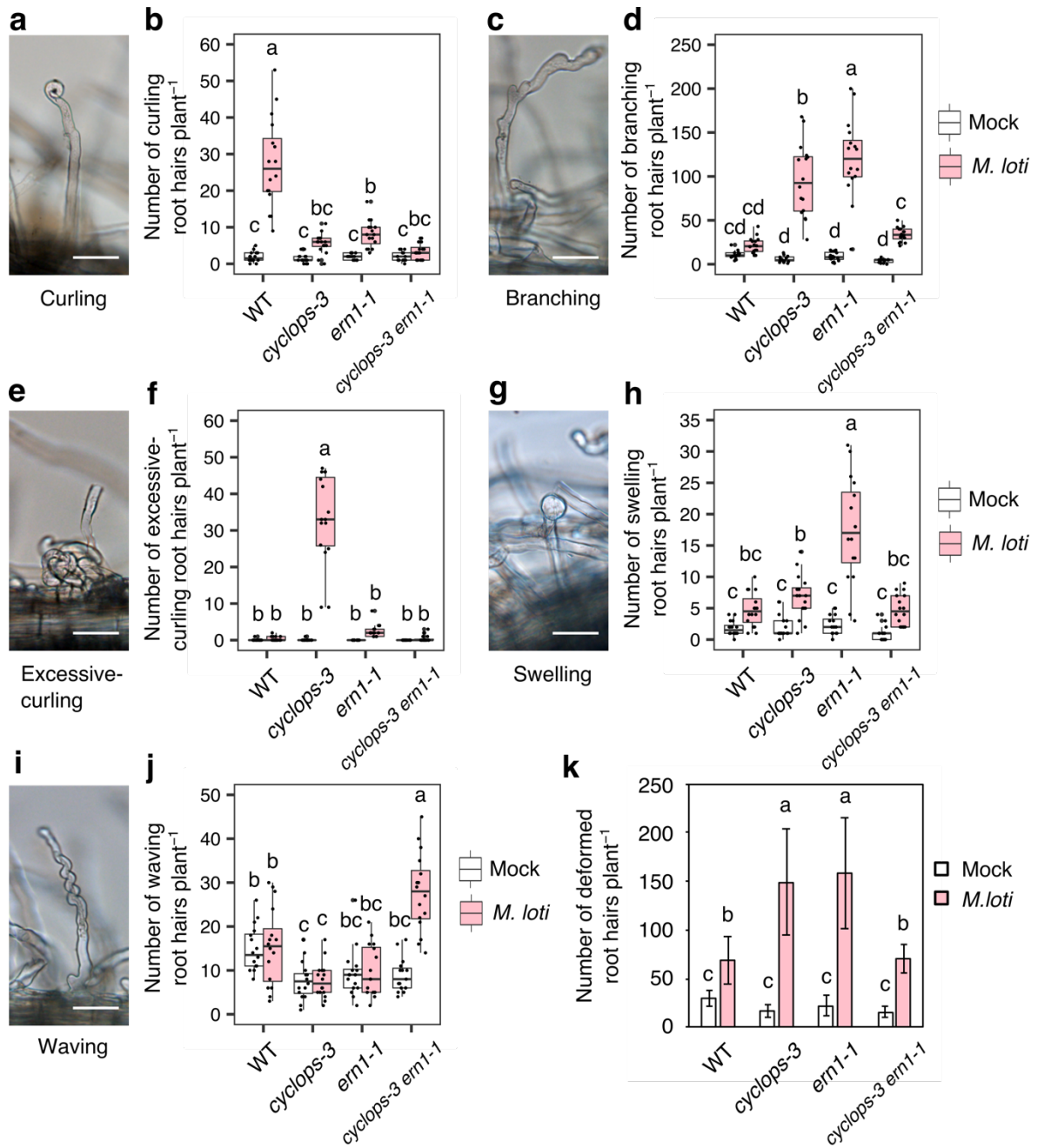
**Figure 8 Symbiotic root hair response of the *cyclops-3 ern1-1* double mutant.**

Representative images and statistical data for root hairs exhibiting curling (**a**, **b**), branching (**c**, **d**), excessive-curling (**e**, **f**), swelling (**g**, **h**), and waving (**i**, **j**) are shown. (**k**) The average number of root hairs exhibiting morphological changes in (**b**, **d**, **f**, **h**, **j**) was calculated. Seven-day-old seedlings were inoculated with mock (white box or bar) or DsRed-labeled *M. loti* (pink box or bar); 16 roots were analyzed at 5 dpi. Scale bar = 50 μm. Boxplots show

statistical analysis of each root hair morphology type. Black dots are actual data points. ANOVA followed by Tukey's HSD test was used for statistical analysis ($P < 0.05$). Error bars in (**k**) indicate SD.
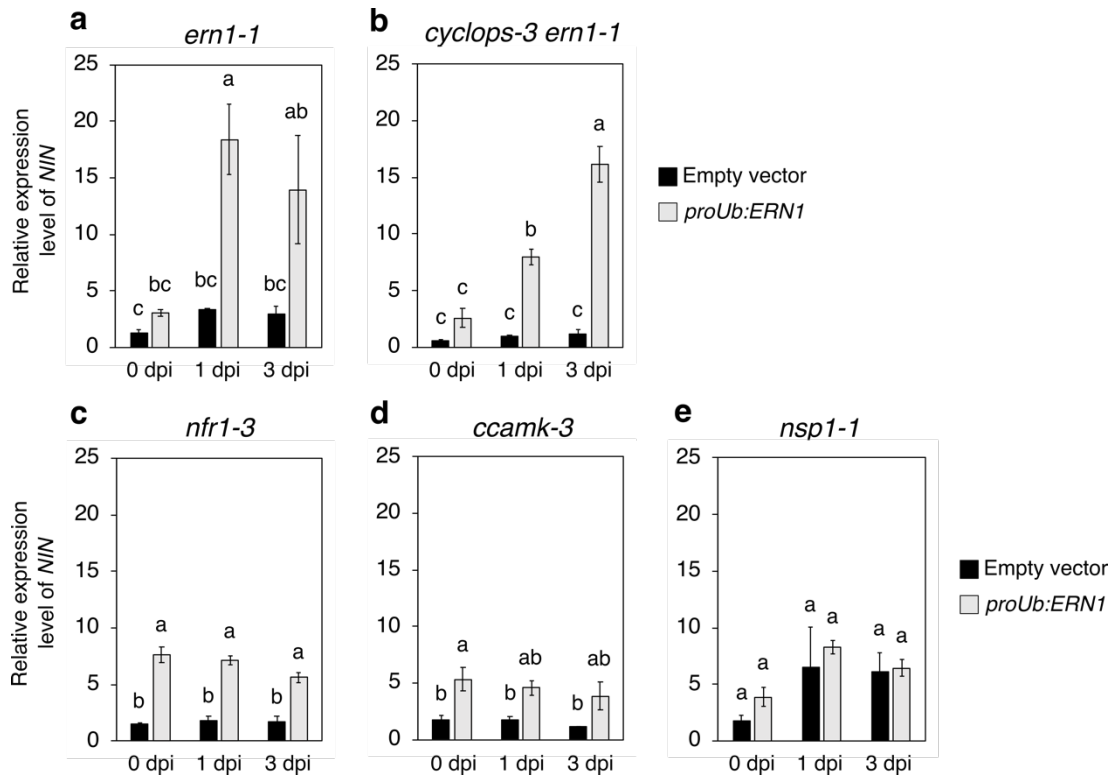
**Figure 9 Effect of ectopic expression of *ERN1* on *NIN* expression.**

Relative expression levels of *NIN* were analyzed by qRT-PCR in *ern1-1* (**a**), *cyclops-3 ern1-1* (**b**), *nfr1-3* (**c**), *ccamk-3* (**d**), and *nsp1-1* (**e**). Roots transformed with an empty vector (black bar) or *proUb:ERN1* (gray bar) were inoculated with mock or *M. loti* MAFF303099. Data are the average of fold changes normalized to *Ubiquitin* and displayed relative to the empty vector control of *ern1-1* at 0 dpi. Error bars indicate SE ($n = 3$, sample size = 12 plants). Statistical analysis was performed by ANOVA followed by Tukey's HSD test ($P < 0.05$).
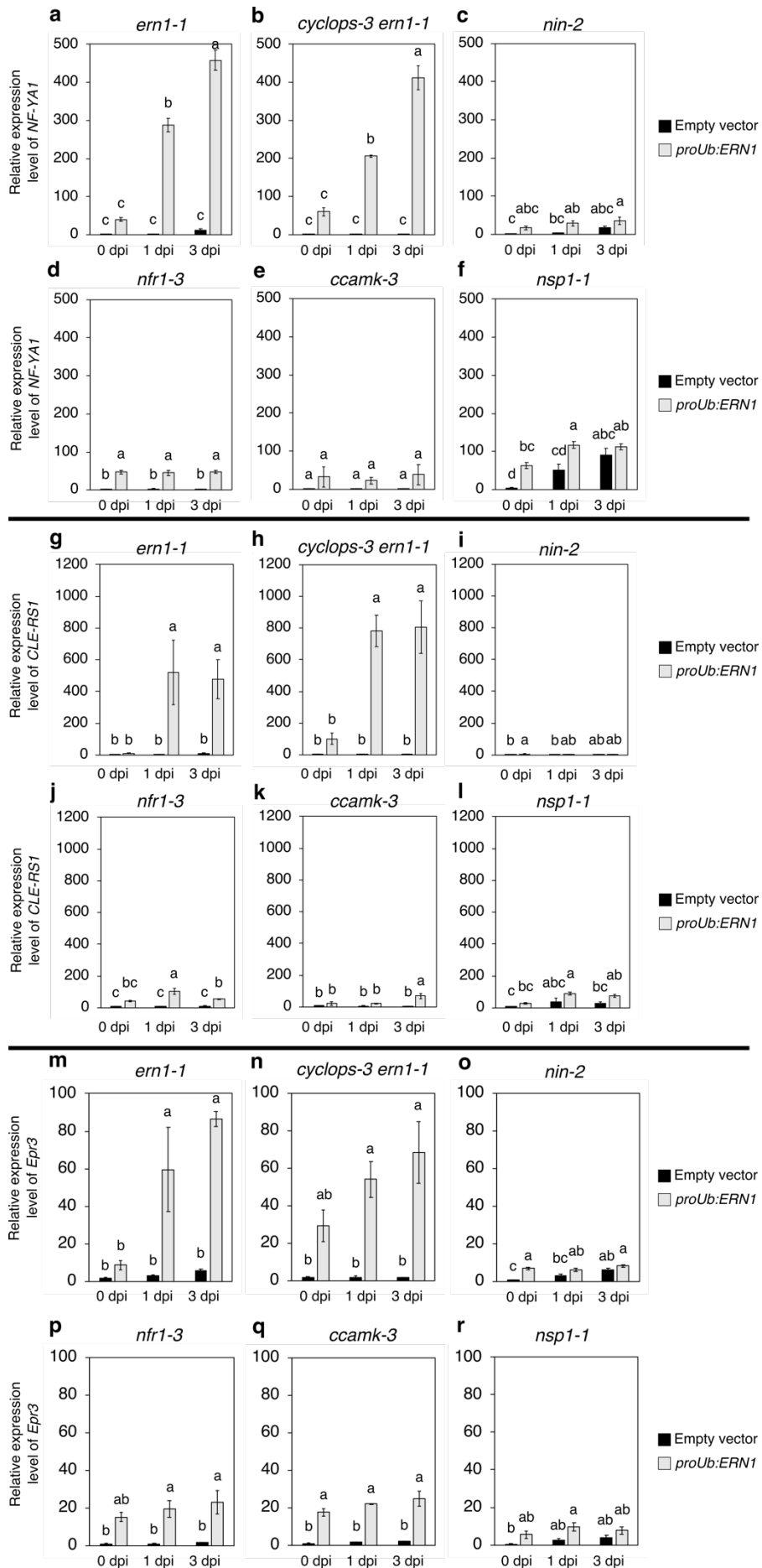
**Figure 10 Effect of ectopic expression of *ERN1* on expression of NIN target genes.**

qRT-PCR analyses of *NF-YA1* (**a−f**), *CLE-RS1* (**g−l**), and *Epr3* (**m−r**) expression in *ern1-1* (**a**, **g**, **m**), *cyclops-3 ern1-1* (**b**, **h**, **n**), *nin-2* (**c**, **i**, **o**), *nfr1-3* (**d**, **j**, **p**), *ccamk-3* (**e**, **k**, **q**), and *nsp1-1* (**f**, **l**, **r**). RNA samples were the same as those used in Figure 9. Data are the average fold change normalized to *Ubiquitin* and displayed relative to the empty vector control of *ern1-1* at 0 dpi. Error bars indicate SE ($n = 3$, sample size = 12 plants). Statistical analysis was performed using ANOVA followed by Tukey's HSD test ($P < 0.05$).
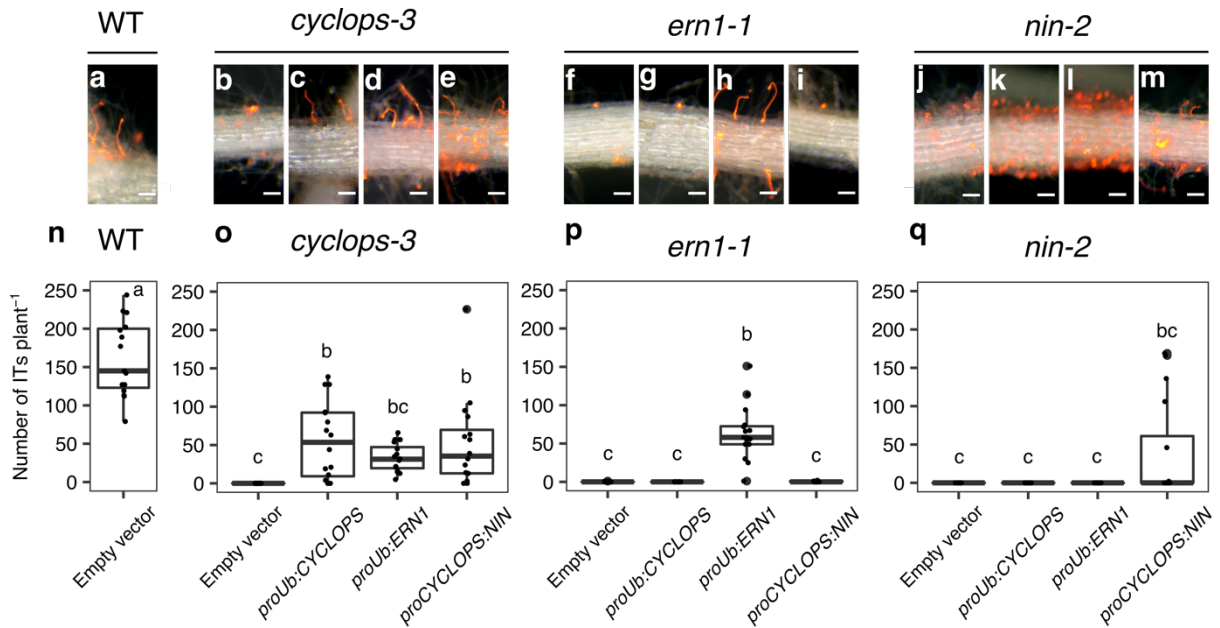
**Figure 11 Functional complementation analysis of symbiotic mutants with ectopic expression of *CYCLOPS*, *ERN1*, and *NIN*.**

(**a–m**) Epidermal phenotypes of WT (Gifu B-129; **a**), *cyclops-3* (**b–e**), *ern1-1* (**f–i**), and *nin-2* (**j–m**) hairy roots carrying empty vector (**a**, **b**, **f**, **j**), *proUb:CYCLOPS* (**c**, **g**, **k**), *proUb:ERN1* (**d**, **h**, **l**), and *proCYCLOPS:NIN* (**e**, **i**, **m**). (**n–q**) Number of ITs in WT (**n**), *cyclops-3* (**o**), *ern1-1* (**p**), and *nin-2* (**q**) roots transformed with the indicated constructs at 14 dpi. Scale bar = 200 μm. For statistical analysis of IT formation, 16 plants were observed per experiment. Dots in (**n–q**) represent actual data points. ANOVA followed by Tukey's HSD test was used to determine the statistical significance across WT (**n**) and three mutants (**o–q**; $P < 0.05$).
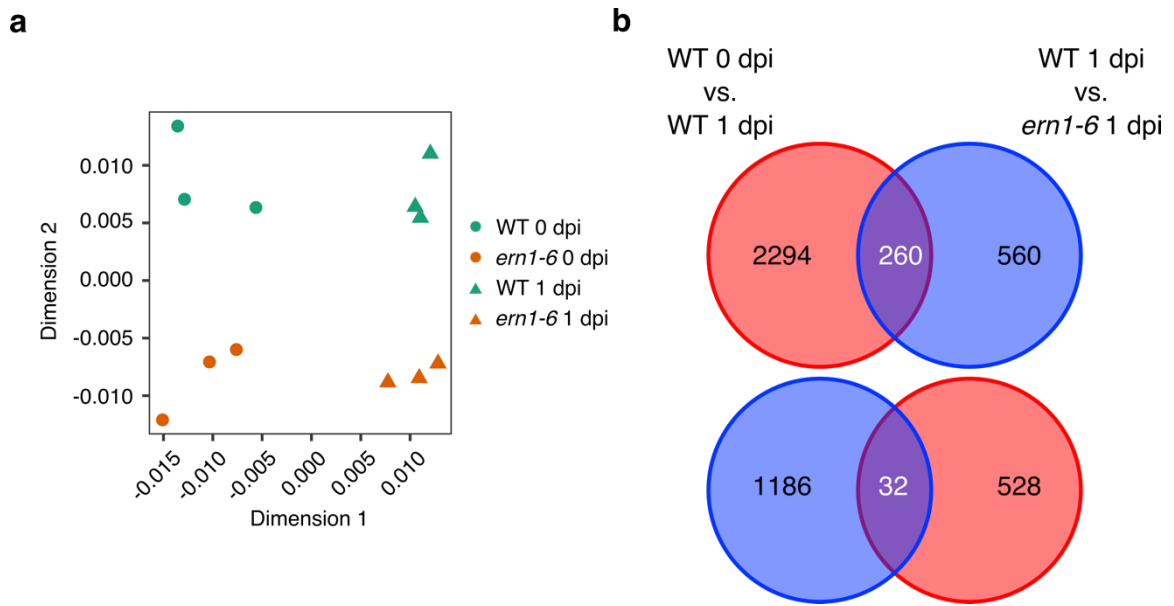
**Figure 12 DEGs detected by RNA-seq in WT (MG-20) and *ern1-6*.**

(**a**) PCA analysis of the effect of rhizobial infection on WT and *ern1-6*. (**b**) Venn diagrams showing number of DEGs detected by RNA-seq. Left circles, DEGs in WT in response to rhizobial infection; right circles, DEGs in *ern1-6* compared with WT after infection. Red circle, up-regulated DEGs; blue circle, down-regulated DEGs. DEGs were defined as FC > 1.5, FDR < 0.1.
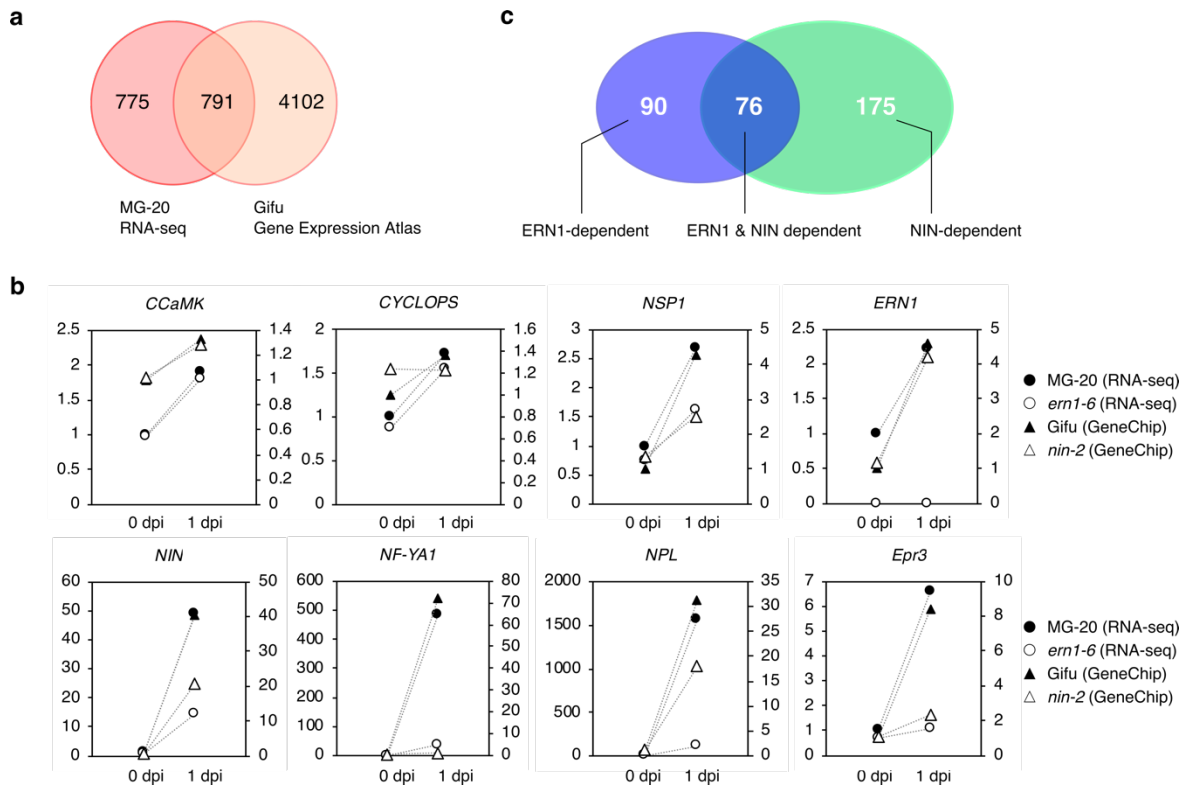
**Figure 13 Gene expression patterns in RNA-seq and Gene Expression Atlas datasets**

(**a**) Venn diagram showing comparison between RNA-seq dataset and Gene Expression Atlas. Among 2554 infection-induced DEGs, 1566 genes were detected in the Atlas. Of the 1566 genes, 791 genes showed an infection-induced expression pattern. (**b**) Fold change of representative symbiotic genes in MG20 and *ern1-6* from the RNA-seq dataset (left *y*-axis), and in Gifu and *nin-2* from the Gene Expression Atlas dataset (right *y*-axis). (**c**) Venn diagram showing numbers of DEGs that are dependent or independent of ERN1 and NIN.
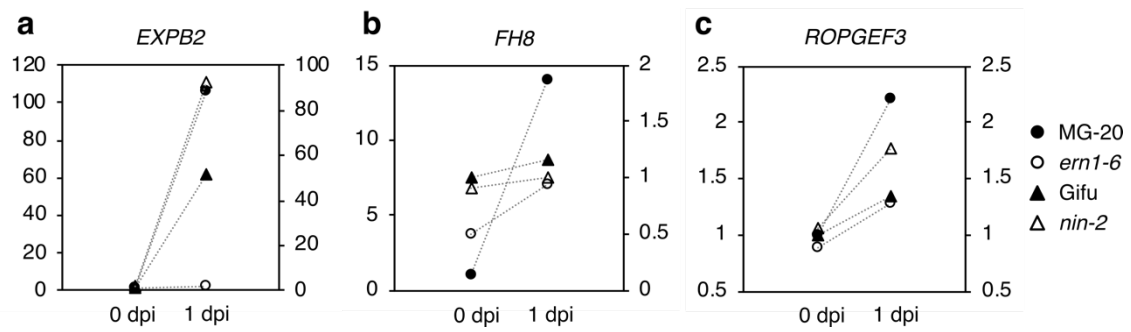
**Figure 14 Expression level of potential ERN1 targets detected by RNA-seq.**

Fold change of *EXPB2* (**a**), *FH8* (**b**), and *ROPGEF3* (**c**) in the RNA-seq dataset (left *y*-axis)

and the Gene Expression Atlas (right *y*-axis).

**Table 1 DEGs down-regulated in *ern1-6* and *nin-2***

| Category | Gene ID | FC in *ern1-6* | FC in *nin-2* | Annotation |
|---|---|---|---|---|
| Cell wall | Lj2g3v1014150 | 0.02 | 0.06 | CASP-like protein N24 |
| | Lj0g3v0306419 | 0.07 | 0.57 | NPL |
| Cytokinin | Lj5g3v0692300 | 0.46 | 0.69 | CKX3 |
| Defense | Lj2g3v0435450 | 0.65 | 0.62 | Multi antimicrobial extrusion protein |
| | Lj5g3v2027290 | 0.65 | 0.62 | Multi antimicrobial extrusion protein |
| | Lj1g3v0627590 | 0.09 | 0.64 | protein PLANT CADMIUM RESISTANCE 2-like |
| DNA/RNA binding | Lj6g3v0326350 | 0.09 | 0.34 | guanine nucleotide-binding protein alpha-2 subunit |
| | Lj6g3v0326360 | 0.10 | 0.34 | guanine nucleotide-binding protein alpha-2 subunit |
| | Lj1g3v4317580 | 0.15 | 0.32 | non-structural maintenance of chromosomes element 4 homolog A-like |
| | Lj2g3v0855300 | 0.60 | 0.18 | probable RNA-dependent RNA polymerase 5 |
| | Lj1g3v1062540 | 0.58 | 0.60 | RNA-binding protein 38-like |
| Early nodulin | Lj4g3v2618530 | 0.09 | 0.05 | aquaporin nip1-2 |
| | Lj4g3v2618540 | 0.09 | 0.05 | aquaporin nip1-2 |
| | Lj0g3v0010149 | 0.06 | 0.22 | early nodulin 5 |
| | Lj4g3v1983610 | 0.03 | 0.22 | early nodulin 5 |
| Electron transport | Lj0g3v0066019 | 0.02 | 0.55 | glutaredoxin-like family |
| | Lj1g3v1786130 | 0.02 | 0.55 | glutaredoxin-like family |
| Enzyme | Lj1g3v2994540 | 0.38 | 0.33 | 2,O-methyltransferase |
| | Lj5g3v0526340 | 0.45 | 0.59 | Acidic mammalian chitinase |
| Enzyme | Lj3g3v0950730 | 0.02 | 0.56 | APN1 |

| | | | | |
|---|---|---|---|---|
| Enzyme | Lj0g3v0185849 | 0.38 | 0.33 | Isoliquiritigenin 2'-O-methyltransferase |
| | Lj0g3v0346019 | 0.05 | 0.59 | isoliquiritigenin 2'-O-methyltransferase |
| | Lj3g3v3751920 | 0.03 | 0.53 | pectinesterase inhibitor 4-like |
| | Lj3g3v3751930 | 0.03 | 0.53 | pectinesterase inhibitor 4-like |
| | Lj4g3v0620030 | 0.08 | 0.27 | PI-PLC X domain-containing protein At5g67130-like |
| | Lj4g3v0620060 | 0.08 | 0.27 | PI-PLC X domain-containing protein At5g67130-like |
| | Lj6g3v1901340 | 0.46 | 0.64 | S-adenosylmethionine decarboxylase |
| | Lj4g3v2253780 | 0.21 | 0.02 | SERPIN,Protease inhibitor I4 |
| | Lj5g3v0465980 | 0.24 | 0.37 | Spermidine/spermine synthases family |
| Gibberellins | Lj0g3v0106899 | 0.47 | 0.31 | GA3 |
| Protein kinase | Lj2g3v1415410 | 0.16 | 0.28 | Epr3 |
| | Lj5g3v2063140 | 0.54 | 0.28 | Inositol-tetrakisphosphate 1-kinase |
| | Lj6g3v2130160 | 0.49 | 0.68 | Protein kinase |
| | Lj2g3v0636810 | 0.39 | 0.50 | Putative LRR receptor-like serine/threonine-protein kinase |
| | Lj0g3v0095039 | 0.23 | 0.65 | Serine-threonine/tyrosine-protein kinase catalytic domain |
| TF | Lj5g3v2063130 | 0.11 | 0.41 | agamous-like MADS-box protein AGL62 |
| | Lj5g3v0841080 | 0.08 | 0.02 | NF-YA1 |
| | Lj4g3v2365210 | 0.29 | 0.41 | NF-YB18 |
| | Lj5g3v1083950 | 0.17 | 0.38 | protein LIGHT-DEPENDENT SHORT HYPOCOTYLS 4-like |
| | Lj6g3v1931790 | 0.30 | 0.15 | PUCHI |
| | Lj0g3v0245069 | 0.60 | 0.41 | transcription factor bHLH30 |
| | Lj4g3v3016310 | 0.38 | 0.13 | Transcription factor MYBS3 |

| Transporter | Lj0g3v0008099 | 0.37 | 0.29 | Cationic amino acid transporter |
|---|---|---|---|---|
| | Lj1g3v2001820 | 0.37 | 0.29 | Cationic amino acid transporter |
| | Lj2g3v0694690 | 0.57 | 0.61 | RING FINGER CONTAINING PROTEIN |
| | Lj6g3v1537040 | 0.30 | 0.12 | CBS-domain |
| | Lj4g3v3113850 | 0.52 | 0.58 | IRK-interacting protein |
| | Lj4g3v3113860 | 0.53 | 0.58 | IRK-interacting protein |
| | Lj0g3v0015379 | 0.16 | 0.17 | plant/F12B17-70 protein |
| | Lj2g3v1728960 | 0.27 | 0.45 | Sec14p-like phosphatidylinositol transfer family protein |

**Table 2 DEGs down-regulated in *ern1-6* but not *nin-2***

| Category | Gene ID | FC in *ern1-6* | FC in *nin-2* | Annotation |
|---|---|---|---|---|
| Actin | Lj1g3v0416320 | 0.50 | 0.87 | FH8 |
| Auxin | Lj2g3v3222870 | 0.27 | 1.21 | IAMT1 |
| Cell wall | Lj1g3v3631760 | 0.02 | 1.79 | EXPB2 |
| CP450 | Lj2g3v3149350 | 0.58 | 1.28 | cytochrome P450 716B1-like |
| | Lj6g3v0778680 | 0.64 | 0.87 | cytochrome P450 71D11 |
| | Lj6g3v0778670 | 0.63 | 1.01 | putative cytochrome P450 |
| Cytokinin | Lj0g3v0068199 | 0.48 | 1.29 | LOG4 |
| Defense | Lj0g3v0203979 | 0.35 | 1.08 | disease resistance protein (TIR-NBS-LRR class) |
| | Lj1g3v3218000 | 0.25 | 1.18 | heat shock cognate 70 kDa protein 2 |
| | Lj3g3v2983920 | 0.36 | 0.96 | Hs1pro-1-like protein |
| | Lj6g3v1038780 | 0.47 | 1.00 | Lipoxygenase2; JA defense related |
| | Lj6g3v2170750 | 0.44 | 1.93 | PR-1-like |
| | Lj1g3v3718130 | 0.37 | 1.08 | Toll/interleukin-1 receptor homology (TIR) domain |
| DNA/RNA binding | Lj0g3v0163209 | 0.54 | 1.25 | NAD(P)-binding domain; GDHRDH,Glucose/ribitol dehydr |
| | Lj0g3v0101689 | 0.49 | 1.13 | NAD(P)-binding Rossmann-fold domains |
| | Lj1g3v4691670 | 0.43 | 1.25 | replication factor A protein 1-like |
| | Lj3g3v2921000 | 0.41 | 1.25 | replication factor A protein 1-like |
| | Lj5g3v2057460 | 0.46 | 2.75 | RETROVIRUS POLYPROTEIN |
| | Lj2g3v1988950 | 0.29 | 0.90 | Reverse transcriptase |
| | Lj2g3v2089570 | 0.35 | 0.92 | SUN domain-containing protein 5 |
| Early nodulin | Lj5g3v0878400 | 0.13 | 0.97 | Nodulin 26 like |
| Enzyme | Lj0g3v0254789 | 0.16 | 1.22 | Legume lectin |
| | Lj0g3v0207589 | 0.62 | 0.90 | 2OG-Fe(II) oxygenase |
| | Lj2g3v1536270 | 0.48 | 0.87 | 4-coumarate--CoA ligase-like 6 |
| | Lj4g3v1683160 | 0.47 | 1.14 | all-alpha NTP pyrophosphatases |

| | | | | |
|---|---|---|---|---|
| Enzyme | Lj1g3v4694380 | 0.54 | 1.22 | glucomannan 4-beta-mannosyltransferase 9 |
| | Lj0g3v0346469 | 0.60 | 0.82 | Oxoglutarate/iron-dependent dioxygenase |
| | Lj2g3v1415420 | 0.08 | 0.84 | peroxidase 28-like |
| | Lj2g3v2411360 | 0.65 | 1.06 | Plant peroxidase |
| | Lj0g3v0320499 | 0.10 | 1.04 | probable pectinesterase 29 |
| | Lj0g3v0306689 | 0.58 | 0.88 | Protein phosphatase 2C-like |
| | Lj2g3v0636030 | 0.47 | 1.05 | SERPIN-RELATED,Protease inhibitor I4 |
| | Lj4g3v2253610 | 0.29 | 1.00 | SERPIN,Protease inhibitor I4 |
| | Lj0g3v0180199 | 0.33 | 1.40 | Short-chain dehydrogenase/reductase |
| | Lj0g3v0254059 | 0.02 | 1.11 | spermidine coumaroyl-CoA acyltransferase-like |
| | Lj0g3v0074289 | 0.21 | 0.84 | Transferase |
| | Lj1g3v2896180 | 0.51 | 0.96 | UDP-glucuronosyl/UDP-glucosyltransf |
| | Lj0g3v0118899 | 0.62 | 1.17 | UDP-glucuronosyl/UDP-glucosyltransferase |
| | Lj1g3v2896160 | 0.61 | 0.96 | UDP-glycosyltransferase 74G1 |
| | Lj2g3v2352610 | 0.51 | 1.06 | UDP-Glycosyltransferase/glycogen phosphorylase |
| F-box | Lj0g3v0214639 | 0.52 | 0.81 | F-box protein |
| Membrane | Lj1g3v2659360 | 0.58 | 1.31 | ROPGEF3 |
| Protein binding | Lj4g3v0336320 | 0.03 | 0.97 | FK506-binding protein 4-like |
| | Lj1g3v2253690 | 0.56 | 0.86 | syringolide-induced protein 14-1-1 |
| Protein kinase | Lj0g3v0088019 | 0.54 | 1.19 | Lectin receptor-like kinase |
| | Lj0g3v0329609 | 0.38 | 1.04 | receptor like protein 21-like |
| | Lj6g3v1370740 | 0.58 | 1.07 | Serine/Threonine protein kinases |
| TF | Lj5g3v2013870 | 0.44 | 1.18 | LAF1 |

| | | | | |
|---|---|---|---|---|
| TF | Lj5g3v2013880 | 0.42 | 1.18 | LAF1 |
| | Lj4g3v0668200 | 0.58 | 0.88 | LBD4 |
| | Lj3g3v2887010 | 0.27 | 0.83 | Myb-related protein Myb4 |
| | Lj0g3v0117029 | 0.20 | 1.13 | probable WRKY transcription factor 61 |
| | Lj5g3v2099560 | 0.18 | 0.93 | transcription factor bHLH84-like |
| Transporter | Lj0g3v0219089 | 0.09 | 0.97 | MtN21 |
| | Lj2g3v0126250 | 0.01 | 1.03 | MtN21 |
| | Lj3g3v1855670 | 0.07 | 0.97 | MtN21 |
| | Lj3g3v1855560 | 0.01 | 1.03 | MtN21 |
| | Lj6g3v0484140 | 0.30 | 1.26 | MATE EFFLUX FAMILY PROTEIN |
| | Lj3g3v2681670 | 0.14 | 0.93 | protein NRT1/ PTR FAMILY 8.1-like |
| | Lj0g3v0331139 | 0.39 | 1.13 | GAG-POL-RELATED RETROTRANSPOSON |
| | Lj3g3v2848790 | 0.14 | 0.95 | GAG-POL-RELATED RETROTRANSPOSON |
| | Lj1g3v2910590 | 0.58 | 1.11 | Leucine rich repeat 4 |
| | Lj0g3v0340399 | 0.30 | 0.91 | LINE-type retrotransposon |
| | Lj3g3v2769460 | 0.49 | 1.51 | QWRF motif-containing protein 3 |
| | Lj0g3v0340359 | 0.37 | 0.81 | RING-H2 finger protein ATL18 |
| | Lj0g3v0336849 | 0.67 | 1.11 | ruBisCO-associated protein-like |
| | Lj0g3v0167879 | 0.52 | 0.78 | SCARECROW-like protein |
| | Lj5g3v0104790 | 0.61 | 1.02 | Transposon protein, putative |
| | Lj0g3v0007899 | 0.50 | 1.06 | Transposon Ty3-I Gag-Pol polyprotein |
| | Lj0g3v0157049 | 0.61 | 1.02 | Zinc finger |

# 4. DISCUSSION

## 4.1 Overlapping and independent functions of *CYCLOPS* and *ERN1* in the symbiotic root hair response

I investigated relationships among *CYCLOPS*, *ERN1*, and *NIN*, which encode transcription factors essential for rhizobial infection processes. Although *ERN1* is a direct target of CYCLOPS, the phenotype analysis of *cyclops-3 ern1-1* indicated that these two factors do not merely act in the same pathway. The *cyclops-3 ern1-1* double mutations affected the symbiotic response more severely than the single mutations alone. Both *cyclops-3* and *ern1-1* generated a few infection threads and a moderate number of micro-colonies in response to rhizobial infection, whereas the double mutants showed a complete lack of infection threads and few micro-colonies (Figure 7). The double mutant also failed to produce nodule primordia, as was observed in the single mutants. This additive phenotype of the double mutant suggests that *CYCLOPS* and *ERN1* have different roles in regulating infection thread formation in addition to common biological functions postulated by the CYCLOPS-mediated *ERN1* transcriptional regulation in *L. japonicus*.

A considerable number of branched root hairs were commonly observed in the single mutants after inoculation with rhizobia (Figure 8). This phenotype implies that *CYCLOPS* and *ERN1* have closely associated functions. However, detailed observation of root hair morphology highlighted the different phenotypes of *cyclops-3* and *ern1-1* mutants. Many root hairs observed in the *cyclops-3* mutant after rhizobial infection were excessively curled, whereas root hairs with a balloon-like shape were often observed in the *ern1-1* mutant. In wild-type plants treated with Nod factors or rhizobial inoculation, the tip of the growing root hair undergoes depolarization, followed by re-initiation of apical growth (Miller et al. 1999). The balloon-shaped root hairs of *ern1-1* might have been arrested at the depolarization stage,

implying that *ERN1* is involved in the re-initiation of tip growth. On the other hand, the root hair phenotype of the *cyclops-3* mutant suggested that *CYCLOPS* is dispensable for root hair curling but is necessary to prevent excessive tip growth. *CYCLOPS* and *ERN1* seem to perform different biological functions and/or contribute differentially to processes involved in root hair deformation. In addition, the total number of deformed root hairs was reduced in the double mutant compared with those of the single mutants, suggesting that root hairs of the double mutant were less sensitive to infection than those of single mutants with regard to morphological changes. These results suggested that *ERN1* functions were independent of the CYCLOPS-mediated transcriptional regulation.

## 4.2 Promotion of infection thread development by ERN1 and its effect on *NIN* expression

The *ern1-1* and *cyclops-3* mutations repressed *NIN* expression that was induced in response to rhizobial infection (Figure 3). Their additive influence on *NIN* expression observed in the *cyclops-3 ern1-1* double mutant indicates that, in addition to *CYCLOPS*, *ERN1* is also involved in the regulation of *NIN* expression in *L. japonicus*. Furthermore, *ERN1* overexpression increased the *NIN* transcript level not only in *ern1-1* but also in *cyclops-3 ern1-1* in the presence of rhizobia (Figure 9). Thus, *ERN1* can contribute to *NIN* expression independently of CYCLOPS. Furthermore, CYCLOPS and ERN1 exerted different effects on *NIN* response to cytokinin. *NIN* expression was up-regulated by exogenous application of cytokinin to the wild-type level in *cyclops-3*, but this induction was affected at an early stage in *ern1-1* (Figure 5). Therefore, ERN1 contributes more effectively than CYCLOPS in regulating *NIN* expression in cytokinin signaling.

The ERN1-mediated regulation of the *NIN* expression level coincided with results obtained from the functional complementation analysis of the infection thread-defective

*cyclops-3* phenotype. Most infection events in *cyclops-3* root hairs were observed as micro-colonies (Yano et al. 2008), indicating that this mutant can recognize nodulation signals but cannot initiate infection thread formation. The epidermal phenotype of *cyclops-3* was rescued by ectopic expression of *ERN1* and *NIN* (Figure 11). Both factors are sufficient for infection thread initiation and elongation in *cyclops-3* root epidermis. However, ectopic expression of *CYCLOPS* did not lead to infection thread formation in *ern1-1* or *nin-2*. Hence, *CYCLOPS* requires *ERN1* and *NIN* to regulate infection thread formation. These results are in accordance with the previously proposed molecular model in which *ERN1* and *NIN* function immediately downstream of *CYCLOPS* in *L. japonicus* (Singh et al. 2014; Cerri et al. 2017). The present results also suggest that *ERN1* and *NIN* function in the same signaling pathway for infection thread formation. In addition, ERN1 has the ability to increase the *NIN* expression level depending on infection (Figure 9). Taking this finding into account, ERN1 suppresses the infection thread-deficient phenotype of *cyclops-3* by increasing the *NIN* expression level. This concept is consistent with the finding that the *nin-2* phenotype was not suppressed by ectopic expression of *ERN1*.

According to this scenario, *NIN* expression under the *CYCLOPS* promoter should restore infection thread formation in the *ern1-1* mutant. However, ectopic expression of *NIN* failed to suppress the epidermal phenotype of *ern1-1* (Figure 11), which was indicative of the requirement for *ERN1*. The more severe phenotype of *cyclops-3 ern1-1* than that of the *cyclops-3* mutant indicated that expression of *ERN1* in the latter single mutant still influenced the symbiotic root hair response (Figure 7; Yano et al. 2017). This expression would be sufficient for *NIN* expression under the *CYCLOPS* promoter to suppress the infection thread-deficient *cyclops* phenotype. In addition, it could be postulated that ERN1 plays a role in regulating the symbiotic root hair response in parallel with the NIN-mediated pathway. This idea is consistent with the different symbiotic root hair phenotypes of *ern1*

and *nin* mutants (Schauser et al. 1999; Marsh et al. 2007; Middleton et al. 2007; Cerri et al. 2016 and 2017; Yano et al., 2017; Kawaharada et al. 2017b).

## 4.3 Requirement of NSP1 for ERN1-mediated *NIN* expression

Although the influence of the *ern1* mutation on *NIN* expression differs among leguminous species, *NIN* transcript accumulation in roots overexpressing *ERN1 in L. japonicus* depends on conserved factors acting in the early nodulation signaling network. Constitutive overexpression of *L. japonicus ERN1* requires rhizobial inoculation to increase expression levels of *NIN* and its transcriptional targets. The lack of induction of these genes in *nfr1-3*, *ccamk-3*, and *nsp1* (Figures 9, 10) indicates that Nod factor signaling is necessary. It could be speculated that Nod factor signaling modulates the transcriptional activity of ERN1 at the protein level. However, unlike CYCLOPS, modification of ERN1 in plant cells is not necessary for its binding to core recognition sequences and transcriptional activity (Kawaharada et al. 2017a).

The requirement of *NSP1* for the effect of *ERN1* on *NIN* expression implies that *ERN1* or its transcriptional targets positively influence the NSP1-mediated pathway. Although the transcriptional activation of *NIN* has not yet been demonstrated, NSP1 binds with NODULATION RESPONSIVE ELEMENTs in the *NIN* promoter together with NSP2 (Hirsch et al. 2009). Previous authors have proposed that NSP1 constitutes large transcription factor complexes with DELLA, CYCLOPS, and NF-YA1 through direct interaction with NSP2 in *M. truncatula* (Hirsch et al., 2009; Fonouni-Farde et al. 2016; Jin et al. 2016). Given that NSP1, CYCLOPS, and NF-YA1 recognize specific nucleotide sequence motifs, variation among NSP1-containing large transcription factor complexes may depend on the components and their target genes. DELLA and NSP1 regulate expression of different genes at a certain stage of the arbuscular mycorrhizal symbiosis

depending on the components in transcription factor complexes (Floss et al. 2017). It is possible that ERN1 regulates components in NSP1-containing transcription factor complexes responsible for the CYCLOPS-independent expression of *NIN*, which possesses multiple regulatory regions in its promoter (Hirsch et al. 2009; Singh et al. 2014; Liu et al. 2019).

## 4.4 Transcriptome analysis of *ern1-6* mutant

Comparison of transcription data between the *ern1-6* and *nin-2* mutants showed that 46% of DEGs (76 of 166 genes) in *ern1-6* were dependent on both *ERN1* and *NIN*. One of the known symbiotic genes in this overlapping subset was *Epr3*. The promoter of *Epr3* is directly targeted and activated by ERN1 and NIN. *Epr3* is probably a common target of ERN1 and NIN. However, qRT-PCR analysis showed that ERN1 did not increase the expression level of *Epr3* in *nin-2* after infection (Figure 10). This result suggests that both ERN1 and NIN are required for regulation of *Epr3* expression and some of their common targets.

The RNA-seq analysis detected three potential downstream genes of *ERN1* that may be involved in root hair growth regulation, namely *EXPB2*, *FH8*, and *RopGEF3*. Expansins mediate auxin-induced cell wall loosening in plants. β-expansin was originally identified as a group-1 allergen from grass pollen. Expansins are secreted at the tip of the pollen tube for loosening of the stigma and style walls. It is hypothesized that expansins cause transient release of short segments of matrix glycans attached to cellulose microfibrils, making cellulose and matrix polymers slide relative to one another (Cosgrove 1998). In *Glycine max*, overexpression of *EXPB2* increases root hair density and infection thread numbers (Li et al. 2015). In *Pisum sativum*, an expansin-like protein is localized in the cell wall of infection threads, suggesting it plays a role in infection thread growth (Sujkowska et al. 2007). *Lotus*

*japonicus EXPB2* may be involved in promoting root hair growth and infection thread formation through loosening of the cell wall, although the exact function remains unclear.

Formins and RopGEFs are involved in actin regulation. Plant formins are suggested to work as membrane anchors for actin polymerization. Formins are able to nucleate and elongate actin filaments or cap the barbed end of actin filament to prevent polymerization (van Gisbergen and Bezanilla 2013). *FH3* knock-down results in swelling of the tip of pollen tubes in *Arabidopsis* (Ye et al. 2009). *Arabidopsis* FH8 is localized in the cell membrane. Mutations in *FH8* inhibit root hair elongation (Deeks et al. 2005). RopGEFs promote activation of *ROP* small GTPases, which regulate the $Ca^{2+}$ gradient, actin dynamics, and other processes required for root hair and pollen tube growth (Pan et al. 2015). Knock-down of RopGEF2 inhibits root hair elongation in *M. truncatula* (Riely et al. 2011). Given that actin cytoskeletal structures are dynamically changed during root hair deformation (Norbert et al. 1998), reduction in the expression levels of *L. japonicus FH8* and *RopGEF3* in *ern1* may affect correct root hair morphology.

In summary, in the present study I showed that, in addition to *CYCLOPS*, *ERN1* positively influences expression of *NIN* dependent on *NSP1*. Both ERN1 and NIN were sufficient to induce infection thread formation in the *cyclops* mutant. This finding was consistent with transcriptional hierarchies demonstrated by results in this study and the model proposed by other researchers. Furthermore, common and independent subsets of ERN1 and NIN downstream genes suggested that the two factors show coordinative and distinct functions. ERN1 constitutes a complex transcriptional network with CYCLOPS and NIN, and contributes to robust regulation of infection processes that ensure strict symbiotic relationships between host legumes and compatible rhizobia.

# 5. CONCLUDING REMARKS

This study set out to explore the missing links among CYCLOPS, ERN1, and NIN. Figure 15 shows a schematic illustration of the model proposed in this study. These three transcription factors function in a complex transcriptional network.

I showed that ERN1 is a positive regulator of *NIN* expression in response to rhizobial infection in *L. japonicus*. ERN1 and NIN also share a number of common downstream genes. This model differs from that proposed for *M. truncatula*, in which ERN1 and NIN are clustered in two independent regulons based on transcription network analysis (Liu et al. 2019). This difference may be due to variation in transcription networks between *L. japonicus* and *M. truncatula*. *Medicago truncatula* ERN1 is able to complement the *L. japonicus ern1* phenotype. This finding suggests that the function of ERN1 is conserved in the two species.

The difference in ERN1−NIN relationship between *L. japonicus* and *M. truncatula* may reflect a transcription "rewiring" during evolution. Dalal and Johnson (2015) proposed that although the output of transcription regulation is often conserved, the underlying network can be very different, i.e., the connection between transcription factors and targets rewire in different species. One example is the Sterol-Regulatory Element Binding Protein (SREBP), a bHLH transcription factor that regulates expression of sterol synthesis genes. SREBP is conserved in many fungi, such as *Cryptococcus neoformans* and *Schizosaccharomyces pombe*. However, the role of SREBP is partially replaced by UPC2, a zinc finger transcription factor, in *Yarrowia lipolytica*. SREBP retains a minor role in sterol synthesis and functions in filamentous growth. However, in *Saccharomyces cerevisiae*, UPC2 has assumed transcriptional regulation of sterol synthesis genes from SREBP, which only functions in filamentation (Maguire et al. 2014). Although the regulatory network for gene expression has changed, the sterol synthesis is not affected. Transcription rewiring

results from the gain and loss of *cis*-regulatory sequences on targets, duplication of transcription factors encoding genes, and "handoff" of targeting genes from one transcription factor to its associated factor (Johnson 2017). Despite the difference in the transcriptional relationship, *ern1* and *nin* mutants in *L. japonicus* exhibited respective phenotypes similar to those of *M. truncatula* counterparts. The transcriptome analysis conducted in *M. truncatula* identified genes downstream of ERN1 and NIN, including *NPL*, expansin, *MtN21*, and *TIR-NBS-LRR*. These homologs were also detected in datasets from *ern1-6* or *nin-2* in *L. japonicus*. Given that the *cis*-element recognized by ERN1 is a short GCC-like sequence, it is expected that the presence of DNA sequences similar to the *cis*-element easily leads to ERN1 rewiring to different targets. Most transcription rewiring may be neutral during evolution, but may sometimes generate new functions if the transcription factor is incorporated into a different network and influence the output phenomena beneficial for the organism. Comparative studies with other legumes are needed to confirm whether the difference in the ERN1−NIN relationship reflects a transcriptional rewiring that occurred during evolution, and whether it is beneficial to regulate infection processes for establishing the symbiotic relationship.
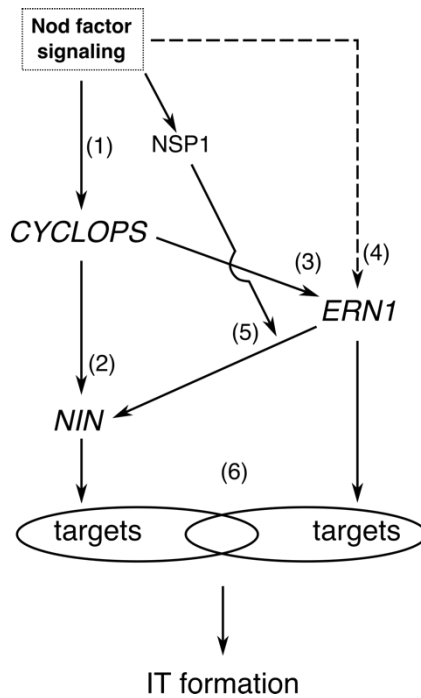
**Figure 15 Schematic illustration of the model for the CYCLOPS−ERN1−NIN transcriptional network proposed in this study.**

CYCLOPS is activated by nodulation signals (1) and directly induces expression of *NIN* (2) and *ERN1* (3) through binding to their promoters. The additive phenotype of *cyclops-3 ern1-1* suggests that unknown factors other than CYCLOPS also contribute to *ERN1* expression and confer the CYCLOPS-independent function on ERN1 in regulating root hair deformation (4). ERN1 also positively influences *NIN* expression dependent on *NSP1* after rhizobial infection (5). ERN1 and NIN regulate expression of their specific and common target genes to promote infection thread formation (6). Solid arrows represent positive regulation determined by previous studies (Messinese et al. 2007; Yano et al. 2008; Xie et al. 2012; Soyano et al. 2013; Singh et al. 2014; Soyano et al. 2014; Qiu et al. 2015; Cerri et al. 2017; Kawaharada et al. 2017b; Liu et al. 2019) and suggested in the present study. A dashed arrow represents a presumed transactivation pathway.

# 6. MATERIAL AND METHODS

**Plant materials and growth conditions**

*L. japonicus* accessions Gifu B-129 and Miyakojima MG-20 were used as the wild type (WT). The *ern1-1* mutant was obtained from the *LORE1* insertion lines (Plant ID, 30034615; Małolepszy et al. 2016) and backcrossed with wild-type Gifu B-129 twice. The mutant lines used in this study, *ern1-1*, *ccamk-3*, *cyclops-3*, *nfr1-3*, *nin-2*, and *nsp1-1*, were generated in the Gifu B-129 background. *ern1-5* and *ern1-6* were generated in the Miyakojima MG-20 background. These mutants were described in previous reports (Schauser et al. 1999; Kawaguchi et al. 2002; Heckmann et al. 2006; Sandal et al. 2006; Yano et al. 2008 and 2017; Kawaharada et al. 2017b).

*L. japonicus* seeds were scarified and surface-sterilized in 10% NaClO (0.2% Tween-20). After soaking overnight in sterile water, the seeds were sown in hydroponic bottles containing 1/2 B5 medium and germinated in growth chamber at 24°C (first day, 24 hr dark; next 3 days, 16 hr light / 8 hr dark). Five-day-old seedlings were transferred to culture vessels containing sterilized vermiculite with B&D medium (Broughton and Dilworth 1971), grown for 2 days for adaptation, and inoculated with *M. loti* MAFF303099 (DsRed-labeled for microscopy observation; Maekawa et al. 2009) or treated with cytokinin (10 nM 6-benzylaminopurine; 6-BA).

**Vector construction**

Primers used for plasmid construction are listed in Table 3. The plasmids were generated using standard techniques and the Gateway Cloning system (Thermo Fisher Scientific). Plasmids used in GUS expression analyses were constructed as follows. The *LjNF-YA1* promoter region, and the *ERN1* promoter and terminator regions were PCR-amplified from

the MG-20 genomic DNA using the PrimeSTAR® GXL DNA polymerase (Takara) and specific primers. The *LjNF-YA1* promoter was inserted between the *Sal*I and *Not*I restriction sites of the pENTR-1A vector (Invitrogen), and then transferred into the pMDC162-GFP vector (Soyano et al. 2013) by the LR reaction (Thermo Fisher Scientific). The *ERN1* promoter, *GUS*, and *ERN1* terminator were sequentially inserted between the *Sal*I and *Xho*I sites of pENTR-1A. The resultant reporter cassette was transferred into pCambia-DC-GFP, a pCambia vector carrying *pro35S:GFP* and a destination cassette. The *proNIN:GUS* construct has been described previously (Soyano et al. 2013). For construction of the entry clones of *ERN1* cDNA and the *NIN* genomic fragment, the sequences were amplified by PCR from the Gifu B-129 cDNA library and genomic DNA. The *ERN1* cDNA was cloned into the pENTR/D-TOPO vector (Thermo Fisher Scientific). The *NIN* genomic fragment was inserted into pENTR-1A after digestion with *Kpn*I and *Not*I. *ERN1* and *CYCLOPS* in the entry vector (Yano et al. 2008) were transferred into pUb-GW-GFP (Maekawa et al. 2008) by the LR reaction. The *NIN* genomic fragment was transferred into pCYCLOPS-GW (Yano et al. 2008).

**Hairy root transformation**

*L. japonicus* seeds were germinated in hydroponic bottles containing 1/2 B5 medium for 4 days (3 days in the dark and 1 day in 16 hr light / 8 hr dark). Hypocotyl cuttings were produced by excising the upper part of each seedling in the middle of the elongated hypocotyl. The hypocotyl cuttings were soaked in suspensions of *A. rhizogenes* AR1193 carrying the corresponding vectors and cultured on co-cultivation medium (B5 medium with Gamborg B5 vitamins solution and 1% agar) in growth chamber at 24°C in the dark for 3 days. Infected shoots were transferred to root induction medium (1/2 B5 medium with 1% sucrose, Gamborg B5 vitamins solution, 12.5 μg mL$^{-1}$ Meropen and 1% agar), grown for

10–15 days (16 hr light / 8 hr dark), and transferred to sterilized vermiculite containing B&D medium. The hairy roots were inoculated with rhizobia 5 days after transfer to vermiculite.

**qRT-PCR analysis of gene expression**

To prepare total RNA from hairy roots, roots expressing GFP as a transformation marker were selected. Whole *L. japonicus* roots were collected for total RNA extraction using PureLink Plant RNA reagents (Invitrogen). The total RNA was treated with DNase I (Takara) to remove genomic DNA, and cDNA was synthesized from 0.5 μg of total RNA using ReverTra Ace qPCR RT Master Mix (Toyobo). The reactions were diluted 10-fold and used as templates for qPCR analysis. The qPCR was performed with Thunderbird SYBR qPCR Mix (Toyobo) on a Roche LightCycler 96 system with the following conditions: 95°C for 90 sec; 42 cycles of 95°C for 10 sec, 55–57°C for 10 sec and 72°C for 30 sec; followed by melting curve analysis. Expression levels were normalized to either *Ubiquitin* or *ATP synthase* and calculated using the ΔΔCt method. The primer sequences are listed in Table 3.

**GUS staining assay**

Roots were washed with 100 mM NaPO$_4$ buffer (pH 7.0). After vacuum infiltration for 10 min, roots were incubated in GUS staining solution [100 mM NaPO$_4$ (pH 7.0), 0.5 mg mL$^{-1}$ 5-bromo-4-chloro-3-indolyl-b-glucuronic acid, 2 mM K$_4$Fe(CN)$_6$, 2 mM K$_3$Fe(CN)$_6$, and 0.1% Triton X-100] for 2−4 h at 37°C.

**Microscopy observation**

Symbiotic phenotypes were observed under a SZX16 fluorescence stereomicroscope and a BX50 fluorescence upright microscope (Olympus). Bright-field and fluorescent images were captured and merged using cellSense Standard software version 1.6 (Olympus).

**Statistical analysis and image generation**

Statistical analysis was performed using R (ver. 3.4.1; R Core Team 2017). Student's *t*-test (unpaired) and Mann−Whitney *U* test were used for single comparisons as indicated. ANOVA followed by Tukey's HSD test was used to determine the statistical significance in multiple group comparisons ($P < 0.05$). For all analyzed data, the normality and homogeneity of variance were checked using the Shapiro−Wilk test and Levene's test before applying Student's *t*-test or ANOVA (agricolae package; De Mendiburu 2017).

Microscopic images and statistical plots were generated with ImageJ (ver. 1.52a; Schneider et al. 2012), the ggplot2 package in R (Wickham 2009), and Inkscape (ver. 0.91; Albert et al. 2015).

**RNA sequencing**

Seven-day-old plants were inoculated with *M. loti* MAFF303099. Twenty roots were sampled at 0 and 1 dpi for each individual biological replicate. Total RNA was isolated using the RNeasy Plant Mini Kit (QIAGEN). Genomic DNA was removed by treatment with DNase (QIAGEN). The integrity of the RNA sample was determined with a bioanalyzer (Agilent). A sample (350 ng) of RNA from each replicate was used for library preparation. Library construction was performed using the NEBNext® Ultra™ II RNA Library Prep Kit for Illumina (NEB) and the NEBNext® Poly(A) mRNA Magnetic Isolation Module (NEB). The concentration of the library was measured using a bioanalyzer (Agilent). RNA sequencing was conducted on an Illumina HiSeq 2000 platform by single-end sequencing (read length = 50 bp) with three independent biological replicates. For dataset analysis, 66 bp of each sample were trimmed and aligned to the *L. japonicus* genome assembly (v3.0) using Tophat2 (v2.1.0; Kim et al. 2013). Raw counts were analyzed using HTseq (v0.6.0;

Anders et al. 2015). DEGs were analyzed with edgeR (v3.18.1; McCarthy et al. 2012).

BLAST and GO annotations were analyzed using Blast2GO (Götz et al. 2008).

**Table 3 Nucleotide sequence of primers**

| Gene | Fwd. sequence (5' - 3') | Rev. sequence (5' - 3') |
|---|---|---|
| (Primers for gene expression analysis) | | |
| *Ubiquitin* | ACGGCTCTTATCAAGGGACCA | CACTTGAGGTGGTTGTAGAGG |
| *CLE-RS1* | TGCAAGTGTCGATGCTCATAGC | GATGTTTTGCTGAACCAAGGGATA |
| *Epr3* | GTCTTCAGCGGGGTATTTGA | TGGCAGCAGTTTTGAACAAG |
| *NF-YA1* | GAAGCTGCTTCAACCTTAAAGTC | CGAGATGTAGAACTGAACTTGTCAC |
| *NIN* | AGCAAAGAGCATTGGTGTATGT | AGCACCCTGCACTGAATCAA |
| *NPL* | CCACATTGCTGGAGGGCCTTG | GCTCACGTACCCACTGCCAC |
| (Primers for vector construction) | | |
| *ERN1* promoter | AAGTCGACTAGTAACTAAGGAAACGTTACTAGC | AAGAATTCACAAATTGTTCAAATTTAGTAATTGAGTGAG |
| *ERN1* | CACCATGGAGATTCAATTCCAGCAACCAA | TTAACAGAACAATGAGCACAAGGGT |
| *ERN1* terminator | AAGCGGCCGCACTTGATCTTGAAGGTCTTAAGTTAATGAT | AACTCGAGATGTGATTATTCTCTTGTAGTTGATGAG |
| *GUS* | AAGAATTCATGGTGTTACGTCCTGTAGAAACCCCA | AAGCGGCCGCTCATTGTTTGCCTCCCTGCTG |
| *NF-YA1* promoter | AAGTCGACCTACAGAATAGGATCTGTGTGAAAC | AAGCGGCCGCGTCTAGGGATTAGGCTCCAAAATG |
| *NIN* | AAGGTACCAAATGGAATATGGTTCATTACTAGTGCAGC | AAGCGGCCGCTTAAGATGGGCTGCTATTGCGGAAT |

# 7. REFERENCES

Albert M, Andler JA, Bah T, Barbry-Blot P, Barraud JF, Barton C, Baxter B, Beard J, Bintz
J, Biro A, Bishop N, Blocher JL, Böck H, Boczkowski T, Bohre H, Boldewyn,
Borgmann D, Bouclet B, Breuer H, Broberg G, Brown C, Brubaker M, Bruno L,
Buculei N, Byak B, Caclin P, Caldwell I, Carmichael G, Catmur E, Celorio C, Cenoz
JA, Ceuppens J, Chyla Z, Clausen A, Cliff J, Cook K, Cromwell B, Crosbie R, Cruz
J, De-Cooman A, Derezynski M, Díaz D, Dilly B, Doolittle L, Dufour N, Dwyer T,
Dziumanenko MV, Engelen J, Erdelyi M, Erikson U, Falzon N, Felfe F, Fitzsimon A,
Flick E, Floryan M, Fowler B, Fred, Gemy C, Giannini S, Gondouin O, Gould T, De
Greef T, Grosberg M, De Gussem K, Harrington B, Harvey D, Heckert AA,
Hetherington C, Hirth J, Hochreiner H, Holder T, Holdsworth J, Holmstedt C, Horkan
A, Hufthammer KO, Hughes R, Hurst N, inductiveload, Ingham T, Irisson JO,
Jamison B, Janeczko T, jEsuSdA, Jurema FL, Kaplinski L, Kerby L, Kiirala N,
Kilfiger J, Kitaev N, Kivlighn J, Knoth A, Kosiński K, Kovar P, Lavorata B, Leone
A, Leray J, Levien R, van Lierop D, Lindgren N, Lipatov V, Louette I, Marc PA,
Marmion AA, Marquardt C, Marshall C, Masár I, Mastrukov DG, Mathog D,
Matiphas, Meeks M, Mena F, MenTaLguY, Monnier A, Montagne V, Mooney T,
Moore DP, Morgan C, Moulder P, Müller J, Nakai Y, Navez V, Neumair C, Nick,
Nilsson A, Oka M, Oliveira VS, Owens M, Penner A, Petroff M, Phillips J, Podobny
Z, Prokoudine A, Reinhard JR, Remizov A, Rodrigo F, Rodrigues H, Rudsatz J, Rueda
XC, Sanches FCS, Schaller C, Scholten M, Von Schwerdtner T, Šegan D, Sharma A,
Shivaken, Sloan M, Smith J, Špetič B, Spike A, Sridharan K, Stephan R, Stojek D,
Sucha M, Suwalski P, Taraben A, Tebby H, Termeau J, Turner D, Twupack A,
Urošević A, Valavanis A, Verona J, Vieites L, Wagenaar D, White LP, Wüst S,
Wybrow M, Xg G, Yacob D, Yamato M, Yip D (2015) Inkscape. http://inkscape.org/.

Amor BB, Shaw SL, Oldroyd GED, Maillet F, Penmetsa RV, Cook D, Long SR, Denarie J,
Gough C (2003) The NFP locus of *Medicago truncatula* controls an early step of Nod
factor signal transduction upstream of a rapid calcium flux and root hair deformation.
Plant J 34: 495–506.

Anders S, Pyl PT, Huber W (2015) HTSeq−a Python framework to work with high-
throughput sequencing data. Bioinformatics, 31: 166−169.

Andriankaja WA, Lien BDA, Frances L, Sauviac L, Jauneau A, Barker DG, De Carvalho-
Niebel F (2007) AP2-ERF transcription factors mediate Nod factor-dependent
*MtENOD11* activation in root hairs via a novel *cis*-regulatory motif. Plant Cell 19:
2866−2885.

Ardourel M, Demont N, Debellé F, Maillet F, de Billy F, Promé JC, Dénarié J, Truchet G
(1994) Rhizobium meliloti lipooligosaccharide nodulation factors: different structural
requirements for bacterial entry into target root hair cells and induction of plant
symbiotic developmental responses. Plant Cell 6: 1357–1374.

Beauchemin NJ, Ghodhbane-Gtari F, Furnholm T, Lavenus J, Svistoonoff S, Doumas P,
Bogusz D, Laplaze L, Tisa LS (2015)  Actinorhizal plant root exudates alter the
physiology, surface properties, and plant infectivity of *Frankia*. Biological Nitrogen
Fixation. Wiley-Blackwell, 2015: 357−364.

Binder A, Soyano T, Hayashi M, Parniske M, Radutoiu S (2014) Plant genes involved in symbiotic signal perception/signal transduction. Springer Berlin Heidelberg, pp 59–71.

Broghammer A, Krusell L, Blaise M, Sauer J, Sullivan JT, Maolanon N, Vinther M, Lorentzen A, Madsen EB, Jensen KJ, Roepstorff P, Thirup S, Ronson CW, Thygesen MB, Stougaard J (2012) Legume receptors perceive the rhizobial lipochitin oligosaccharide signal molecules by direct binding. Proc Natl Acad Sci USA 109: 13859–13864.

Catoira R, Galera C, de Billy F, Penmetsa RV, Journet EP, Maillet F, Rosenberg C, Cook D, Gough C, Dénarié J (2000) Four genes of *Medicago truncatula* controlling components of a Nod factor transduction pathway. Plant Cell 12: 1647–1666.

Cerri MR, Frances L, Kelner A, Fournier J, Middleton PH, Auriac MC, Mysore KS, Wen J, Erard M, Barker DG, Oldroyd GE, de Carvalho-Niebel F (2016) The symbiosis-related ERN transcription factors act in concert to coordinate rhizobial host root infection. Plant Physiol 171: 1037−1054.

Cerri MR, Frances L, Laloum T, Auriac MC, Niebel A, Oldroyd GED, Barker DG, Fournier J, de Carvalho-Niebel F (2012) *Medicago truncatula* ERN transcription factors: regulatory interplay with NSP1/NSP2 GRAS factors and expression dynamics throughout rhizobial infection. Plant Physiol 160: 2155–2172.

Cerri MR, Wang Q, Stolz P, Folgmann J, Frances L, Katzer K, Li X, Heckmann AB, Wang TL, Downie JA, Klingl A, de Carvalho-Niebel F, Xie F, Parniske M (2017) The *ERN1* transcription factor gene is a target of the CCaMK/CYCLOPS complex and controls rhizobial infection in *Lotus japonicus*. New Phytol 215: 323−337.

Cosgrove DJ (1998) Update on cell growth cell wall loosening by expansins. Plant Physiol 118: 333–339.

Dalal CK, Johnson AD (2017) How transcription circuits explore alternative architectures while maintaining overall circuit output. Genes Dev 31: 1397−1405.

Deeks MJ, Cvrcková F, Machesky LM, Mikitová V, Ketelaar T, Zársky V, Davies B, Hussey PJ (2005) *Arabidopsis* group Ie formins localize to specific cell membrane domains, interact with actin-binding proteins and cause defects in cell expansion upon aberrant expression. New Phytol 168: 529–540.

De Mendiburu F (2017) agricolae: statistical procedures for agricultural research. R package version 1.2-8. https://CRAN.R-project.org/package=agricolae

Downie JA (2014) Legume nodulation. Curr Biol 24: R184−R190.

Ehrhardt DW, Wais R, Long SR (1996) Calcium spiking in plant root hairs responding to rhizobium nodulation signals. Cell 85: 673–681.

Endre G, Kereszt A, Kevei Z, Mihacea S, Kaló P, Kiss GB (2002) A receptor kinase gene regulating symbiotic nodule development. Nature 417: 962.

Esseling JJ, Lhuissier FGP, Emons AMC (2003) Nod factor-induced root hair curling: continuous polar growth towards the point of Nod factor application. Plant Physiol 132:

1982–1988.

Fisher RF, Long SR (1992) Rhizobium-plant signal exchange. Nature 357: 655–660.

Floss DS, Gomez SK, Park HJ, MacLean AM, Müller LM, Bhattarai KK, Lévesque-Tremblay V, Maldonado-Mendoza IE, Harrison MJ (2017) A transcriptional program for arbuscule degeneration during AM symbiosis is regulated by MYB1. Curr Biol 27: 1206–1212.

Fonouni-Farde C, Tan S, Baudin M, Brault M, Wen J, Mysore KS, Niebel A, Frugier F, Diet A (2016) DELLA-mediated gibberellin signalling regulates Nod factor signalling and rhizobial infection. Nat Commun 7: 12636.

Fournier J, Teillet A, Chabaud M, Ivanov S, Genre A, Limpens E, de Carvalho-Niebel F, Barker DG (2015) Remodeling of the infection chamber before infection thread formation reveals a two-step mechanism for rhizobial entry into the host legume root hair. Plant Physiol 167: 1233–1242.

Fournier J, Timmers ACJ, Sieberer BJ, Jauneau A, Chabaud M, Barker DG (2008) Mechanism of infection thread elongation in root hairs of *Medicago truncatula* and dynamic interplay with associated rhizobial colonization. Plant Physiol 148: 1985–1995.

Gage DJ (2004) Infection and invasion of roots by symbiotic, nitrogen-fixing rhizobia during nodulation of temperate legumes. Microbiol Mol Biol Rev 68: 280–300.

Götz S, García-Gómez JM, Terol J, Williams TD, Nagaraj SH, Nueda MJ, Robles M, Talón M, Dopazo J, Conesa A (2008) High-throughput functional annotation and data mining with the Blast2GO suite. Nucleic acids research, 36: 3420-3435.

Guinel FC, Geil RD (2002) A model for the development of the rhizobial and arbuscular mycorrhizal symbioses in legumes and its use to understand the roles of ethylene in the establishment of these two symbioses. Can J Bot 80: 695–720.

Hayashi T, Banba M, Shimoda Y, Kouchi H, Hayashi M, Imaizumi-Anraku H (2010) A dominant function of CCaMK in intracellular accommodation of bacterial and fungal endosymbionts. Plant J 63: 141−154.

Heckmann AB, Lombardo F, Miwa H, Perry JA, Bunnewell S, Parniske M, Wang TL, Downie JA (2006) *Lotus japonicus* nodulation requires two GRAS domain regulators, one of which is functionally conserved in a non-legume. Plant Physiol 142: 1739–1750.

Heckmann AB, Sandal N, Bek AS, Madsen LH, Jurkiewicz A, Nielsen MW, Tirichine L, Stougaard J (2011) Cytokinin induction of root nodule primordia in *Lotus japonicus* is regulated by a mechanism operating in the root cortex. Mol Plant Microbe Interact 24: 1385–1395.

Hirsch AM (1992) Developmental biology of legume nodulation. New Phytol 122: 211–237.

Hirsch S, Kim J, Munoz A, Heckmann AB, Downie JA, Oldroyd GED (2009) GRAS proteins form a DNA binding complex to induce gene expression during nodulation signaling in *Medicago truncatula*. Plant Cell 21: 545–557.

Ivanov S, Fedorova EE, Limpens E, De Mita S, Genre A, Bonfante P, Bisseling T (2012) Rhizobium-legume symbiosis shares an exocytotic pathway required for arbuscule formation. Prol Natl Acad Sci USA 109: 8316−8321.

Jin Y, Liu H, Luo D, Yu N, Dong W, Wang C, Zhang X, Dai H, Yang J, Wang E (2016) DELLA proteins are common components of symbiotic rhizobial and mycorrhizal signalling pathways. Nat Commun 7: 12433.

Johnson AD (2017) The rewiring of transcription circuits in evolution. Curr Opin Genet Dev 47: 121−127.

Kaló P, Gleason C, Edwards A, Marsh J, Mitra RM, Hirsch S, Jakab J, Sims S, Long SR, Rogers J, Kiss GB, Downie JA, Oldroyd GED (2005) Nodulation signaling in legumes requires NSP2, a member of the GRAS family of transcriptional regulators. Science 308: 1786–1789.

Kang H, Chu X, Wang C, Xiao A, Zhu H, Yuan S, Yang Z, Ke D, Xiao S, Hong Z, Zhang Z (2014) A MYB coiled-coil transcription factor interacts with NSP2 and is involved in nodulation in *Lotus japonicus*. New Phytolol 201: 837−849.

Kawaguchi M, Imaizumi-Anraku H, Koiwa H, Niwa S, Ikuta A, Syono K, Akao S (2002) Root, root hair, and symbiotic mutants of the model legume *Lotus japonicus*. Mol Plant Microbe Interact 15: 17–26.

Kawaharada Y, Kelly S, Nielsen MW, Hjuler CT, Gysel K, Muszyński A, Carlson RW, Thygesen MB, Sandal N, Asmussen MH, Vinther M, Andersen SU, Krusell L, Thirup S, Jensen KJ, Ronson CW, Blaise M, Radutoiu S, Stougaard J (2015) Receptor-mediated exopolysaccharide perception controls bacterial infection. Nature 523: 308–312.

Kawaharada Y, Nielsen MW, Kelly S, James EK, Andersen KR, Rasmussen SR, Füchtbauer W, Madsen LH, Heckmann AB, Radutoiu S, Stougaard J (2017a) Differential regulation of the Epr3 receptor coordinates membrane-restricted rhizobial colonization of root nodule primordia. Nat Commun 8: 14534.

Kawaharada Y, James EK, Kelly S, Sandal N, Stougaard J (2017b) The ERF Required for Nodulation1 (ERN1) transcription factor is required for infection thread formation in *Lotus japonicus*. Mol Plant Microbe Interact 30: 194−204.

Ke D, Fang Q, Chen C, Zhu H, Chen T, Chang X, Yuan S, Kang H, Ma L, Hong Z, Zhang Z (2012) The small GTPase ROP6 interacts with NFR5 and is involved in nodule formation in *Lotus japonicus*. Plant Physiol 159: 131−143.

Kelly S, Radutoiu S, Stougaard J (2017) Legume LysM receptors mediate symbiotic and pathogenic signalling. Curr Opin Plant Biol 39: 152–158.

Kim D, Pertea G, Trapnell C, Pimentel H, Kelley R, Salzberg SL (2013) TopHat2: accurate alignment of transcriptomes in the presence of insertions, deletions and gene fusions. Genome biology, 14: R36.

Kistner C, Parniske M (2002) Evolution of signal transduction in intracellular symbiosis. Trends Plant Sci 7: 511–518.

Kouchi H, Imaizumi-Anraku H, Hayashi M, Hakoyama T, Nakagawa T, Umehara Y, Suganuma N, Kawaguchi M (2010) How many peas in a pod? Legume genes responsible for mutualistic symbioses underground. Plant Cell Physiol 51: 1381–1397.

Laloum T, Baudin M, Frances L, Lepage A, Billault-Penneteau B, Cerri MR, Ariel F, Jardinaud MF, Gamas P, de Carvalho-Niebel F, Niebel A (2014) Two CCAAT-box-binding transcription factors redundantly regulate early steps of the legume-rhizobia endosymbiosis. Plant J 79: 757−768.

Laporte P, Lepage A, Fournier J, Catrice O, Moreau S, Jardinaud MF, Mun JH, Larrainzar E, Cook DR, Gamas P, Niebel A (2014) The CCAAT box-binding transcription factor NF-YA1 controls rhizobial infection. J Exp Bot 65: 481–494.

Larrainzar E, Riely BK, Kim SC, Carrasquilla-Garcia N, Yu HJ, Hwang HJ, Oh M, Kim GB, Surendrarao AK, Chasman D, Siahpirani AF, Penmetsa RV, Lee GS, Kim N, Roy S, Mun JH, Cook DR (2015) Deep sequencing of the *Medicago truncatula* root transcriptome reveals a massive and early interaction between nodulation factor and ethylene signals. Plant Physiol 169: 233–265.

Lévy J, Bres C, Geurts R, Chalhoub B, Kulikova O, Duc G, Journet EP, Ané JM, Lauber E, Bisseling T, Dénarié J, Rosenberg C, Debellé F (2004) A putative $Ca^{2+}$ and calmodulin-dependent protein kinase required for bacterial and fungal symbioses. Science 303: 1361−1364.

Li X, Zhao J, Tan Z, Zeng R, Liao H (2015) GmEXPB2, a cell wall β-expansin gene, affects soybean nodulation through modifying root architecture and promoting nodule formation and development. Plant Physiol 169: 2640−2653.

Limpens E, Franken C, Smit P, Willemse J (2003) LysM domain receptor kinases regulating rhizobial Nod factor. Science 302: 630–634.

Liu CW, Breakspear A, Guan D, Cerri MR, Abbs K, Jiang S, Robson FC, Radhakrishnan G, Roy S, Bone C, Stacey N, Rogers C, Trick M, Niebel A, Oldroyd GE, de Carvalho-Niebel F, Murray JD (2019) NIN acts as a network hub controlling a growth module required for rhizobial infection. Plant Physiol 179: 1704−1722.

Madsen EB, Antolín-Llovera M, Grossmann C, Ye J, Vieweg S, Broghammer A, Krusell L, Radutoiu S, Jensen ON, Stougaard J, Parniske M (2011) Autophosphorylation is essential for the *in vivo* function of the *Lotus japonicus* Nod factor receptor 1 and receptor-mediated signalling in cooperation with Nod factor receptor 5. Plant J 65: 404–417.

Madsen EB, Madsen LH, Radutoiu S, Olbryt M, Rakwalska M, Szczyglowski K, Sato S, Kaneko T, Tabata S, Sandal N, Stougaard J (2003) A receptor kinase gene of the LysM type is involved in legume perception of rhizobial signals. Nature 425: 637–640.

Madsen LH, Tirichine L, Jurkiewicz A, Sullivan JT, Heckmann AB, Bek AS, Ronson CW, James EK, Stougaard J (2010) The molecular network governing nodule organogenesis and infection in the model legume *Lotus japonicus*. Nat Commun 1: 10.

Maekawa T, Kusakabe M, Shimoda Y, Sato S, Tabata S, Murooka Y, Hayashi M (2008)

Polyubiquitin promoter-based binary vectors for overexpression and gene silencing in *Lotus japonicus*. Mol Plant Microbe Interact 21: 375–382.

Maekawa T, Maekawa-Yoshikawa M, Takeda N, Imaizumi-Anraku H, Murooka Y, Hayashi M (2009) Gibberellin controls the nodulation signaling pathway in *Lotus japonicus*. Plant J 58: 183–194.

Maguire SL, Wang C, Holland LM, Brunel F, Neuvéglise C, Nicaud JM, Zavrel M, White TC, Wolfe KH, Butler G (2014) Zinc finger transcription factors displaced SREBP proteins as the major sterol regulators during *Saccharomycotina* evolution. PLoS Genet 10: e1004076.

Małolepszy A, Mun T, Sandal N, Gupta V, Dubin M, Urbański D, Shah N, Bachmann A, Fukai E, Hirakawa H, Tabata S, Nadzieja M, Markmann K, Su J, Umehara Y, Soyano T, Miyahara A, Sato S, Hayashi M, Stougaard J, Andersen SU (2016) The *LORE1* insertion mutant resource. Plant J 88: 306–317.

Marsh JF, Rakocevic A, Mitra RM, Brocard L, Sun J, Eschstruth A, Long SR, Schultze M, Ratet P, Oldroyd GED (2007) *Medicago truncatula* NIN is essential for rhizobial-independent nodule organogenesis induced by autoactive calcium/calmodulin-dependent protein kinase. Plant Physiol 144: 324–335.

McCarthy DJ, Chen Y, Smyth GK (2012). Differential expression analysis of multifactor RNA-Seq experiments with respect to biological variation. Nucleic Acids Research 40: 4288−4297.

Messinese E, Mun JH, Yeun LH, Jayaraman D, Rougé P, Barre A, Lougnon G, Schornack S, Bono JJ, Cook DR, Ané JM (2007) A novel nuclear protein interacts with the symbiotic DMI3 calcium- and calmodulin-dependent protein kinase of *Medicago truncatula*. Mol Plant Microbe Interact 20:912–921.

Middleton PH, Jakab J, Penmetsa RV, Starker CG, Doll J, Kalo P, Prabhu R, Marsh JF, Mitra RM, Kereszt A, Dudas B, VandenBosch K, Long SR, Cook DR, Kiss GB, Oldroyd GED (2007) An ERF transcription factor in *Medicago truncatula* that is essential for Nod factor signal transduction. Plant Cell 19: 1221–1234.

Miller DD, De Ruijter NCA, Bisseling T, Emons AMC (1999) The role of actin in root hair morphogenesis: Studies with lipochito-oligosaccharide as a growth stimulator and cytochalasin as an actin perturbing drug. Plant J 17: 141–154.

Miwa H, Sun J, Oldroyd GED, Downie JA (2006) Analysis of Nod-factor-induced calcium signaling in root hairs of symbiotically defective mutants of *Lotus japonicus*. Mol Plant Microbe Interact 19: 914–923.

Moling S, Bisseling T (2015) Evolution of rhizobium nodulation: From nodule-specific genes (Nodulins) to recruitment of common processes. Biological Nitrogen Fixation, 2: 39.

Mun T, Bachmann A, Gupta V, Stougaard J, Andersen SU (2016) Lotus Base: An integrated information portal for the model legume *Lotus japonicus*. Sci Rep 6:39447.

Murakami E, Cheng J, Gysel K, Bozsoki Z, Kawaharada Y, Hjuler CT, Sørensen KK, Tao

K, Kelly S, Venice F, Genre A, Thygesen MB, de Jong N, Vinther M, Jensen DB, Jensen KJ, Blaise M, Madsen LH, Andersen KR, Stougaard J, Radutoiu S (2018) Epidermal LysM receptor ensures robust symbiotic signalling in *Lotus japonicus*. Elife 7: e33506.

Murakami Y, Miwa H, Imaizumi-Anraku H, Kouchi H, Downie JA, Kawaguchi M, Kawasaki S (2006) Positional cloning identifies *Lotus japonicus* NSP2, a putative transcription factor of the GRAS family, required for *NIN* and *ENOD40* gene expression in nodule initiation. DNA Res 13:255–265.

Murray JD, Karas BJ, Sato S, Tabata S, Amyot L, Szczyglowski K (2007) A cytokinin perception mutant colonized by rhizobium in the absence of nodule organogenesis. Science 315: 101−104.

Norbert CAD, Rook MB, Bisseling T, Emons AMC (1998) Lipochito-oligosaccharides re-initiate root hair tip growth in *Vicia sativa* with high calcium and spectrin-like antigen at the tip. Plant J 13: 341–350.

Okamoto S, Ohnishi E, Sato S, Takahashi H, Nakazono M, Tabata S, Kawaguchi M (2009) Nod factor/nitrate-induced *CLE* genes that drive HAR1-mediated systemic regulation of nodulation. Plant Cell Physiol 50: 67–77.

Oldroyd GED (2013) Speak, friend, and enter: signalling systems that promote beneficial symbiotic associations in plants. Nat Rev Microbiol 11: 252–263.

Oldroyd GED, Downie JA (2008) Coordinating nodule morphogenesis with rhizobial infection in legumes. Annu Rev Plant Biol 59: 519−546.

Oldroyd GED, Long SR (2003) Identification and characterization of *Nodulation-Signaling Pathway 2*, a gene of *Medicago truncatula* involved in Nod actor signaling. Plant Physiol 131: 1027−1032.

Ott T, van Dongen JT, Gu̎nther C, Krusell L, Desbrosses G, Vigeolas H, Bock V, Czechowski T, Geigenberger P, Udvardi MK (2005) Symbiotic leghemoglobins are crucial for nitrogen fixation in legume root nodules but not for general plant growth and development. Curr Biol 15: 531–535.

Pan X, Chen J, Yang Z (2015) Auxin regulation of cell polarity in plants. Curr Opin Plant Biol 28:144–153.

Pawlowski K, Demchenko KN (2012) The diversity of actinorhizal symbiosis. Protoplasma 249: 967–979.

Pimprikar P, Carbonnel S, Paries M, Katzer K, Klingl V, Bohmer MJ, Karl L, Floss DS, Harrison MJ, Parniske M, Gutjahr C (2016) A CCaMK-CYCLOPS-DELLA complex activates transcription of RAM1 to regulate arbuscule branching. Curr Biol 26: 987–998.

Plet J, Wasson A, Ariel F, Le Signor C, Baker D, Mathesius U, Crespi M, Frugier F (2011) MtCRE1-dependent cytokinin signaling integrates bacterial and plant cues to coordinate symbiotic nodule organogenesis in *Medicago truncatula*. Plant J 65: 622–633.

Popp C, Ott T (2011) Regulation of signal transduction and bacterial infection during root nodule symbiosis. Curr Opin Plant Biol 14: 458–467.

Qiu L, Lin J, Xu J, Sato S, Parniske M, Wang TL, Downie JA, Xie F (2015) SCARN a novel class of SCAR protein that is required for root-hair infection during legume nodulation. PLOS Genet 11: e1005623.

Radutoiu S, Madsen LH, Madsen EB, Felle HH, Umehara Y, Grønlund M, Sato S, Nakamura Y, Tabata S, Sandal N, Stougaard J (2003) Plant recognition of symbiotic bacteria requires two LysM receptor-like kinases. Nature 425: 585–592.

R Core Team (2017) R: A language and environment for statistical computing. R Foundation for Statistical Computing, Vienna, Austria. URL https://www.R-project.org/

Riely BK, He H, Venkateshwaran M, Sarma B, Schraiber J, Ané JM, Cook DR (2011) Identification of legume *RopGEF* gene families and characterization of a *Medicago truncatula RopGEF* mediating polar growth of root hairs. Plant J 65: 230–243.

Sandal N, Petersen TR, Murray J, Umehara Y, Karas B, Yano K, Kumagai H, Yoshikawa M, Saito K, Hayashi M, Murakami Y, Wang X, Hakoyama T, Imaizumi-Anraku H, Sato S, Kato T, Chen W, Hossain MS, Shibata S, Wang TL, Yokota K, Larsen K, Kanamori N, Madsen E, Radutoiu S, Madsen LH, Radu TG, Krusell L, Ooki Y, Banba M, Betti M, Rispail N, Skøt L, Tuck E, Perry J, Yoshida S, Vickers K, Pike J, Mulder L, Charpentier M, Müller J, Ohtomo R, Kojima T, Ando S, Marquez AJ, Gresshoff PM, Harada K, Webb J, Hata S, Suganuma N, Kouchi H, Kawasaki S, Tabata S, Hayashi M, Parniske M, Szczyglowski K, Kawaguchi M, Stougaard J (2006) Genetics of symbiosis in *Lotus japonicus* : recombinant inbred lines, comparative genetic maps, and map position of 35 symbiotic loci. Mol Plant Microbe Interact 19: 80–91.

Schauser L, Roussis A, Stiller J, Stougaard J (1999) A plant regulator controlling development of symbiotic root nodules. Nature 402: 191–195.

Schneider CA, Rasband WS, Eliceiri KW (2012) NIH Image to ImageJ: 25 years of image analysis. Nature methods 9: 671-675.

Shimoda Y, Han L, Yamazaki T, Suzuki R, Hayashi M, Imaizumi-Anraku H (2012) Rhizobial and fungal symbioses show different requirements for calmodulin binding to calcium calmodulin-dependent protein kinase in *Lotus japonicus*. Plant Cell 24: 304−321.

Singh S, Parniske M (2012) Activation of calcium-and calmodulin dependent protein kinase (CCaMK), the central regulator of plant root endosymbiosis. Curr Opin Plant Biol 15: 444−453.

Singh S, Katzer K, Lambert J, Cerri M, Parniske M (2014) CYCLOPS, a DNA-binding transcriptional activator, orchestrates symbiotic root nodule development. Cell Host Microbe 15: 139–152.

Smit P, Limpens E, Geurts R, Fedorova E, Dolgikh E, Gough C, Bisseling T (2007) *Medicago* LYK3, an entry receptor in rhizobial nodulation factor signaling. Plant Physiol 145: 183–91.

Smit P, Raedts J, Portyanko V, Debellé F, Gough C, Bisseling T, Geurts R (2005) NSP1 of the GRAS protein family is essential for rhizobial Nod factor-induced transcription. Science 308: 1789−1791.

Soyano T, Hirakawa H, Sato S, Hayashi M, Kawaguchi M (2014) NODULE INCEPTION creates a long-distance negative feedback loop involved in homeostatic regulation of nodule organ production. Proc Natl Acad Sci USA 111: 14607–14612.

Soyano T, Kouchi H, Hirota A, Hayashi M (2013) NODULE INCEPTION directly targets NF-Y subunit genes to regulate essential processes of root nodule development in *Lotus japonicus*. PLoS Genet 9: e1003352.

Stracke S, Kistner C, Yoshida S, Mulder L, Sato S, Kaneko T, Tabata S, Sandal N, Stougaard J, Szczyglowski K, Parniske M (2002) A plant receptor-like kinase required for both bacterial and fungal symbiosis. Nature 417: 959–962.

Sujkowska M, Borucki W, Golinowski W (2007) Localization of expansin-like protein in apoplast of pea (*Pisum sativum L.*) root nodules during interaction with *Rhizobium leguminosarum* bv. *viciae* 248. Acta Societatis Botanicorum Poloniae 76.

Svistoonoff S, Tromas A, Diagne N, Alloisio N, Laplaze L, Champion A, Bogusz D, Bonneau J, Hocher V (2015) How transcriptomics revealed new information on actinorhizal symbioses establishment and evolution. Biological Nitrogen Fixation. Wiley-Blackwell, 2015: 425−432.

Tirichine L, Imaizumi-Anraku H, Yoshida S, Murakami Y, Madsen LH, Miwa H, Nakagawa T, Sandal N, Albrektsen AS, Kawaguchi M, Downie A, Sato S, Tabata S, Kouchi H, Parniske M, Kawasaki S, Stougaard J (2006) Deregulation of a Ca$^{2+}$/calmodulin-dependent kinase leads to spontaneous nodule development. Nature 441: 1153–1156.

Tsyganova AV, Tsyganov VE (2018) Plant genetic control over infection thread development during legume-rhizobium symbiosis. Symbiosis.InechOpen.

van Gisbergen PAC, Bezanilla M (2013) Plant formins: Membrane anchors for actin polymerization. Trends Cell Biol 23:227–233.

van Spronsen PC, Grønlund M, Pacios-Bras C, Spaink HP, Kijne JW (2001) Cell biological changes of outer cortical root cells in early determinate nodulation. Mol Plant Microbe Interact 14: 839–847.

van Zeijl A, Op den Camp RHM, Deinum EE, Charnikhova T, Franssen H, Op den Camp HJM, Bouwmeester H, Kohlen W, Bisseling T, Geurts R (2015) Rhizobium lipo-chitooligosaccharide signaling triggers accumulation of cytokinins in *Medicago truncatula* roots. Mol Plant 8: 1213–1226.

Venkateshwaran M, Jayaraman D, Chabaud M, Genre A, Balloon AJ, Maeda J, Forshey K, den Os D, Kwiecien NW, Coon JJ, Barker DG, Ané JM (2015) A role for the mevalonate pathway in early plant symbiotic signaling. Proc Natl Acad Sci USA 112: 9781–9786.

Voordeckers K, Pougach K, Verstrepen K J (2015) How do regulatory networks evolve and expand throughout evolution? Curr Opin Biotechnol  34: 180−188.

Wickham H (2009) ggplot2: Elegant Graphics for Data Analysis. Springer-Verlag New York.

Xie F, Murray JD, Kim J, Heckmann AB, Edwards A, Oldroyd GED, Downie JA (2012) Legume pectate lyase required for root infection by rhizobia. Proc Natl Acad Sci USA 109: 633−638.

Yano K, Aoki S, Liu M, Umehara Y, Suganuma N, Iwasaki W, Sato S, Soyano T, Kouchi H, Kawaguchi M (2017) Function and evolution of a *Lotus japonicus* AP2/ERF family transcription factor that is required for development of infection threads. DNA Res 24: 193−203.

Yano K, Yoshida S, Mü Ller J, Singh S, Banba M, Vickers K, Markmann K, White C, Schuller B, Sato S, Asamizu E, Tabata S, Murooka Y, Perry J, Wang TL, Kawaguchi M, Imaizumi-Anraku H, Hayashi M, Parniske M (2008) CYCLOPS, a mediator of symbiotic intracellular accommodation. Proc Natl Acad Sci USA 105: 20540-20545.

Ye J, Zheng Y, Yan A, Chen N, Wang Z, Huang S, Yang Z (2009) *Arabidopsis* Formin3 directs the formation of actin cables and polarized growth in pollen tubes. Plant Cell 21: 3868−3884.

Yoshida S, Parniske M (2005) Regulation of plant symbiosis receptor kinase through serine and threonine phosphorylation. J Biol chem 280: 9203−9209.